



**Innovations Deserving
Exploratory Analysis Programs**

NCHRP IDEA Program

Non-Gating Guardrail Terminal

Final Report for
NCHRP IDEA Project 212

Prepared by:
Anth Dean L. Sicking, Ph.D., P.E.
Kevin D. Schrum, Ph.D., P.E.
Kent Walls, Ph.D.
Joe Schwertz, MSBME
Blake Feltman, MSME
Steve Thompsonony J. Alongi
University of Alabama at Birmingham

September 2020

Innovations Deserving Exploratory Analysis (IDEA) Programs Managed by the Transportation Research Board

This IDEA project was funded by the NCHRP IDEA Program.

The TRB currently manages the following three IDEA programs:

- The NCHRP IDEA Program, which focuses on advances in the design, construction, and maintenance of highway systems, is funded by American Association of State Highway and Transportation Officials (AASHTO) as part of the National Cooperative Highway Research Program (NCHRP).
- The Safety IDEA Program currently focuses on innovative approaches for improving railroad safety or performance. The program is currently funded by the Federal Railroad Administration (FRA). The program was previously jointly funded by the Federal Motor Carrier Safety Administration (FMCSA) and the FRA.
- The Transit IDEA Program, which supports development and testing of innovative concepts and methods for advancing transit practice, is funded by the Federal Transit Administration (FTA) as part of the Transit Cooperative Research Program (TCRP).

Management of the three IDEA programs is coordinated to promote the development and testing of innovative concepts, methods, and technologies.

For information on the IDEA programs, check the IDEA website (www.trb.org/idea). For questions, contact the IDEA programs office by telephone at (202) 334-3310.

IDEA Programs
Transportation Research Board
500 Fifth Street, NW
Washington, DC 20001

The project that is the subject of this contractor-authored report was a part of the Innovations Deserving Exploratory Analysis (IDEA) Programs, which are managed by the Transportation Research Board (TRB) with the approval of the National Academies of Sciences, Engineering, and Medicine. The members of the oversight committee that monitored the project and reviewed the report were chosen for their special competencies and with regard for appropriate balance. The views expressed in this report are those of the contractor who conducted the investigation documented in this report and do not necessarily reflect those of the Transportation Research Board; the National Academies of Sciences, Engineering, and Medicine; or the sponsors of the IDEA Programs.

The Transportation Research Board; the National Academies of Sciences, Engineering, and Medicine; and the organizations that sponsor the IDEA Programs do not endorse products or manufacturers. Trade or manufacturers' names appear herein solely because they are considered essential to the object of the investigation.

Non-Gating Guardrail Terminal

IDEA Program Project Final Report

Project NCHRP-212

Prepared for the IDEA Program

Transportation Research Board

The National Academies of Sciences, Engineering and Medicine

by:

Dean L. Sicking, Ph.D., P.E.

Joe Schwertz, MSBME

Kevin D. Schrum, Ph.D., P.E.

Blake Feltman, MSME

Kent Walls, Ph.D.

Steve Thompson

University of Alabama at Birmingham

September 22, 2020

ACKNOWLEDGMENTS

The NCHRP IDEA Program supported this research, with a special thanks to Dr. Inam Jawed for his guidance. The authors also wish to acknowledge Michelle Owens of the Alabama Department of Transportation, Erik Emerson of the Wisconsin Department of Transportation, and Bill Wilson of the Wyoming Department of Transportation for their advice and assistance as members of the panel of advisors for this project. The authors are grateful for their input and revision suggestions for the final report. The text, as embodied herein, includes their suggested edits to help clarify some points.

NCHRP IDEA PROGRAM

COMMITTEE CHAIR

CATHERINE MCGHEE
Virginia DOT

MEMBERS

AHMAD ABU HAWASH
Iowa DOT

FARHAD ANSARI
University of Illinois at Chicago

PAUL CARLSON
Road Infrastructure, Inc.

ALLISON HARDT
Maryland State Highway Administration

ERIC HARM
Consultant

JOE HORTON
California DOT

DENISE INDA
Nevada DOT

DAVID JARED
Georgia DOT

PATRICIA LEAVENWORTH
Massachusetts DOT

MAGDY MIKHAIL
Texas DOT

J. MICHELLE OWENS
Alabama DOT

A. EMILY PARKANY
Virginia Agency of Transportation

JAMES SIME
Consultant

JOSEPH WARTMAN
University of Washington

FHWA LIAISON

MARY HUIE
Federal Highway Administration

TRB LIAISON

RICHARD CUNARD
Transportation Research Board

IDEA PROGRAMS STAFF

CHRISTOPHER HEDGES
Director, Cooperative Research Programs

LORI SUNDSTROM
Deputy Director, Cooperative Research Programs

INAM JAWED
Senior Program Officer

DEMISHA WILLIAMS
Senior Program Assistant

EXPERT REVIEW PANEL

ERIK EMERSON, *Wisconsin DOT*

BILL WILSON, *Wyoming DOT*

MICHELLE OWENS, *Alabama DOT.*

TABLE OF CONTENTS

Acknowledgments.....	i
Table Of Contents	ii
Executive Summary	1
1. Background	2
2. IDEA Product.....	2
3. Concept and Innovation.....	2
4. Investigation	3
4.1. Find Barrier Redirection Literature	3
4.2. Synthesize the Literature	3
4.3. Determine Minimum Redirecting Force.....	5
4.4. Determine Maximum Lateral Compliance	6
4.5. Create Simple Spring Model in LS-Dyna.....	7
4.6. Debug the LS-Dyna Spring/Truck Model	8
4.7. Tuning the Spring Stiffness	8
4.7.1. Single-Variable Parametric Study - Corner Impacts	9
4.7.2. Two-Variable Parametric Study – Quarter-Point Impacts.....	11
4.8. Full-Scale Simulations	13
4.9. Brainstorming Prototype Configurations.....	15
4.10. Crash Test Evaluations of Prototype	16
5. Conclusions	21
6. Plans for Implementation	21
7. Questions from Reviewers	22
8. References	23
9. Appendix A – Results of Single-Variable parameter Study	26
10. Appendix B – Results of Two-Variable parameter Study	30
11. Appendix C – Results of Two-Variable parameter Study	31
12. Appendix D – Research Results	32

EXECUTIVE SUMMARY

Guardrail terminals were first developed in response to frequent spearing on the end of untreated guardrail. Previously, it was thought that such a small point on the roadside would not be struck often enough to warrant consideration. When further data was available, and new systems were developed, the design of the guardrail terminal began its evolution. The first iteration of guardrail end treatments was a turned down system, which was intended to eliminate spearing by turning the end section of w-beam downward and placing the free end on the groundline. While it accomplished the objective of eliminating spearing, it introduced violent rollovers, and as a result the rate of fatal and severe crashes was relatively unaltered. Therefore, the evolution continued with the introduction of the Breakaway Cable Terminal (BCT), which was designed to break off upon impact rather than impale a vehicle. This particular design was shown to be too stiff, resulting in penetrations of the vehicle passenger compartment in later crash test results. As such, the Federal Highway Administration (FHWA) no longer considers the BCT eligible for federal reimbursement. However, its concept was improved upon by other designs, such as the Eccentric Loader Terminal (ELT) and Slotted Rail Terminal (SRT). While these were improvements, they were not evolutionary changes as they were based on the same basic concept as the BCT. The ET-2000, however, was the first terminal to actively absorb the energy of the vehicle, representing a massive paradigm shift in the design of guardrail terminals. Its successors were built upon the same concept: put the rail in compression and deform the rail in order to absorb energy. The X-Tension and SoftStop were then introduced to place the rail in tension while deforming the rail. This evolution was intended to minimize the chance of the guardrail buckling and forming a potential spear tip. However, none of these designs or concepts are capable of preventing a vehicle from gating behind the barrier. When these terminals are struck on the end at a high enough angle (for example, 15 degrees), the guardrail will form a plastic hinge, and a portion of that guardrail will swing open, like a gate, and allow the vehicle to pass behind.

For decades, this gating action has been readily accepted by the highway safety engineering community and has been enshrined in state and federal policies and design guides. For example, the Roadside Design Guide (RDG) (1) provides instruction on calculating the length-of-need (LON) for a compression-based guardrail based on the placement of the hazard, among other things. The beginning of this LON must coincide with the third post of a tangent guardrail terminal, or about 12.5 feet from the end. That is a reference to the fact that when a vehicle strikes the guardrail prior to the third post, the vehicle will gate behind the barrier. However, such a trajectory would keep the vehicle from striking the shielded hazard. Therefore, the RDG includes calculations that account the gating nature of end terminals.

The proposed research seeks to evolve guardrail terminals once more and provide the means whereby a new host of terminals can be developed that act as non-gating devices. The benefits of a non-gating device are clear. There would be less risk to motorists associated with non-linear encroachment paths and high-velocity in off-road conditions. The overall length of guardrail required to shield a hazard would be reduced because the beginning of the LON would be at or near the end of the guardrail terminal. This would save on budgets for State DOTs, minimize exposure of the construction crews to dangerous traffic, and reduce the number of impacts between vehicle and guardrail (which is proportional to the installation length). In other words, a non-gating terminal would cost less in terms of funding and human lives.

Crash tests were investigated through an extensive literature search to identify trends in a guardrail's ability to redirect a vehicle. Then, with this knowledge, simple and complex computer models were created to identify parameters with the greatest influence on preventing gating. The complex model included an actual terminal with a 5,000-lb pickup truck striking the end of the terminal at 15 degrees. This model helped guide the research team in designing, building, and testing a prototype. This prototype was a tension-based system that absorbed the kinetic energy of the vehicle. It was subjected to two full-scale tests. The first was with a Ford Explorer at 50 mph and 15 degrees. This vehicle was chosen for two reasons: (1) availability; and (2) high rollover risk. Given the severe nature of the loading due the angle, and the difficult task of producing a non-gating behavior, a lower speed was selected. In the future, larger vehicles and faster speeds (i.e., MASH pickup at TL-3) will be explored. The second test used a Mazda Protégé at 64 mph and 15 degrees. This test was meant to replicate MASH testing using a small car to ensure that ride down accelerations and vehicle stability were acceptable. In both cases, the forward velocity of the vehicle was stopped while it maintained engagement with the terminal head. In other words, the vehicle did not pass behind and beyond the terminal head at any point. Both tests would have passed all criteria in MASH.

1. BACKGROUND

Guardrail terminals are meant to prevent errant vehicles from rolling over or becoming impaled. They treat the end of a longitudinal W-beam barrier, which is in place to redirect vehicles back to the roadway. Many impacts with the terminal are at high angles. At some critical angle, the guardrail terminal gates open rather than continue to collapse or extrude. Currently, no terminal is capable to preventing this “gating” action entirely. Instead, current terminals open in a controlled manner and allow the vehicle to pass behind the barrier. To accommodate this, the area behind the barrier that the vehicle would encroach upon must be clear. This often extends the Length-Of-Need (LON) of the barrier to provide sufficient shielding of the hazards behind the barrier.

A truly non-gating guardrail terminal will help reduce the overall LON required for the circumstance, compared to traditional compression-based terminals, thus saving money for allocation elsewhere. It would also reduce the severity of errors made by the engineer in determining the size of the clear zone and placement of the terminal with respect to the clear zone. It would help reduce the speed of severe-angle impacts such that when the vehicle overpowers the barrier and gates through (despite the non-gating design), the vehicle will be traveling slower. Slower speeds, of course, correspond to higher degrees of safety, especially once the vehicle has passed behind the barrier.

This study seeks to determine the tools necessary to build a non-gating guardrail terminal. W-beam, the most common longitudinal barrier in the country, has demonstrated decades of success in redirecting vehicles. However, in doing so, it benefits from a developed membrane action that contributes to the barrier’s stiffness. A guardrail end cannot develop the same tension and therefore must create this stiffness in another way.

An engineer can easily design a structure that has a prescribed stiffness. For example, if a barrier needs to supply a stiffness of 10 kips/foot, the engineer can develop a post and beam system that generates 30 kips for 3 feet of lateral movement. However, the actual determination of the design load is far more complicated. This project will accomplish two main objectives: (1) provide the real stiffness needed to redirect a vehicle on the end of a guardrail barrier; and (2) propose a prototype non-gating terminal. With these two objectives met, the industry as a whole will have the tools to work on next-generation terminals and the confidence that their work will succeed.

2. IDEA PRODUCT

W-beam guardrail terminals have undergone numerous transformative evolutions since the 1960s. First, the deadly blunt-end spear tip was removed by a turned down system. Then, the end was weakened so that it would not impale vehicles and did not need to create a ramp. Then, the terminal was used as a means of absorbing energy and slowing the vehicle down. Terminals have historically been compression-based, but now products are emerging that are tensioned-based. The IDEA product described herein is another such development in the long history of guardrail terminal evolution. Terminals have always been considered a gating device, allowing vehicles to pass behind them when struck at a high enough angle and close enough to the end. The result of this IDEA project provides both the tools and understanding necessary to design a non-gating terminal as well as a prototype that proves the concept.

3. CONCEPT AND INNOVATION

The concept behind the proposed non-gating terminal is that there is continuous membrane action supplied by the barrier throughout the duration of the impact. This membrane action exerts a continuous lateral force on the vehicle that works to decelerate the vehicle in the lateral direction while also decelerating the vehicle in the longitudinal direction. In order to accomplish this, there must be a strong connection between the rail and the anchor that remains affixed for all impacts except for crashes from the reverse direction. In addition to this connection, the terminal must absorb the energy of the vehicle by deforming the W-beam guardrail, and a lateral force must be exerted on the vehicle to get it to redirect. The combination of the longitudinal and lateral forces is of critical importance.

The prototype built in this project accomplishes all three functions. First, the cable was outfitted with a swaged button on one end and a threaded rod on the other. The threaded rod was fed through an anchor boot constructed of steel plates and welded to a large wide-flange I-beam. This beam was driven into the ground and included a soil plate to prevent as

much movement as possible. The first guardrail panel was modified to include a rectangular hole in the valley near the end. The swaged button was set into this rectangular opening and welded to the W-beam (prior to galvanization). That connection was reinforced with additional gauge steel welded in place to arrest any cracks that may develop. The cable and modified first panel were passed through the impact head during installation, with the cable being bolted to the anchor boot and tightened.

The longitudinal force used to decelerate the vehicle was generated by an internal structure that folded the W-beam backwards on itself. To do so, a wedge was installed in the head to line up with the valley of the W-beam. Above and below it, two angled plates were placed to interact with the top and bottom edges of the W-beam. As the head moved along the rail, the valley was pushed toward the road while the top and bottom edges were pushed toward the roadside. This folding process created permanent deformation in the steel W-beam. Because of this, a great deal of strain energy was required and was therefore taken from the kinetic energy of the vehicle. The size, shape, and placement of these internal plates were adjustable such that the research team could generate an optimal longitudinal force in concert with the lateral force.

The lateral force was controlled by the cross-section of the posts used in the study. Replacing the standard line post, the research team developed an open-section, rectangular post. This design was fabricated from gauge steel ranging in thickness from 7 ga to 12 ga. The steel was bent into a square shape with a gap included on one leg of the square. The thickness of the metal along with the width and depth were adjustable such that the research team could generate an optimal lateral force in concert with the longitudinal force.

Crash testing done on a prototype developed in this study demonstrated exemplary non-gating performance. The authors' knowledge, no other guardrail terminal has maintained engagement with a vehicle and effectively brought it to a stop when the vehicle struck the terminal at 15 degrees. As such, it is possible that the length-of-need may begin much sooner, relative to the end of the terminal. This would reduce the expense of a longer section of guardrail while still providing the same or greater level of protection.

4. INVESTIGATION

4.1. FIND BARRIER REDIRECTION LITERATURE

Research reports were gathered from the UNL MwRSF research hub. The research team was expressly interested in NCHRP 350 (1) and MASH (3) crash tests conducted at Test Level 3 (TL-3). This test level utilizes a small car and a pickup truck to impact the device at 62.4 mph. The search revealed 47 full-scale crash tests when the search parameters were focused on Test Nos. 10 and 11. Test 10 uses a small car with a nominal weight of 2,425 pounds, while Test 11 uses a pickup truck with a nominal weight of 5,000 pounds. In both tests, the vehicles are oriented at 25 degrees with respect to the guardrail. These tests are referred to as Length-of-Need (LON) tests, meaning that the guardrail is expected to capture and redirect the vehicle safely back to the road from which it departed. In other words, the guardrail does not allow the vehicle to pass behind the barrier, much like a non-gating event.

Some of the 47 full-scale tests identified in the search were for other tests. Often a single report described either Test 10 or 11, but also included other tests such as Test No. 32, 34, 35 and 37. These tests vary the angle and location of initial impact. Of those 47 tests, 28 included guardrail barriers that demonstrated redirection capability. References for each of the crash test results used in this study are provided in (4) through (34).

4.2. SYNTHESIZE THE LITERATURE

When a full-scale crash test report was identified, the filtered acceleration v. time history, typically provided in the appendices of the report, were fed into a MATLAB program developed by the research team. This program treated the acceleration plot as an image and used the number of pixels between the origin and the ends of the axes to create a local conversion system. Then, the analyst clicked on the peaks and valleys of the plot, and each click was read by the program as the (x, y) position of the plot. Finally, the program reproduced the plot based on the clicked input points and also provided the maximum value in the plot. This value was recorded in the database for that test. In the future, this program may be expanded to cover lateral deflections as well, if needed. An example of a real full-scale data plot is shown in FIGURE 1,

with the replicated MATLAB output on top of it. The superimposed MATLAB results are nearly a perfect match. This result was taken from the lateral acceleration of the vehicle in an MGS crash test with a small car (MASH Test No. 3-10). The program indicated that for this test, the peak acceleration was 8.35 G's at 0.20 seconds. For the 2,423-lb vehicle, this acceleration was equivalent to 20,232 pounds of force to redirect the vehicle.

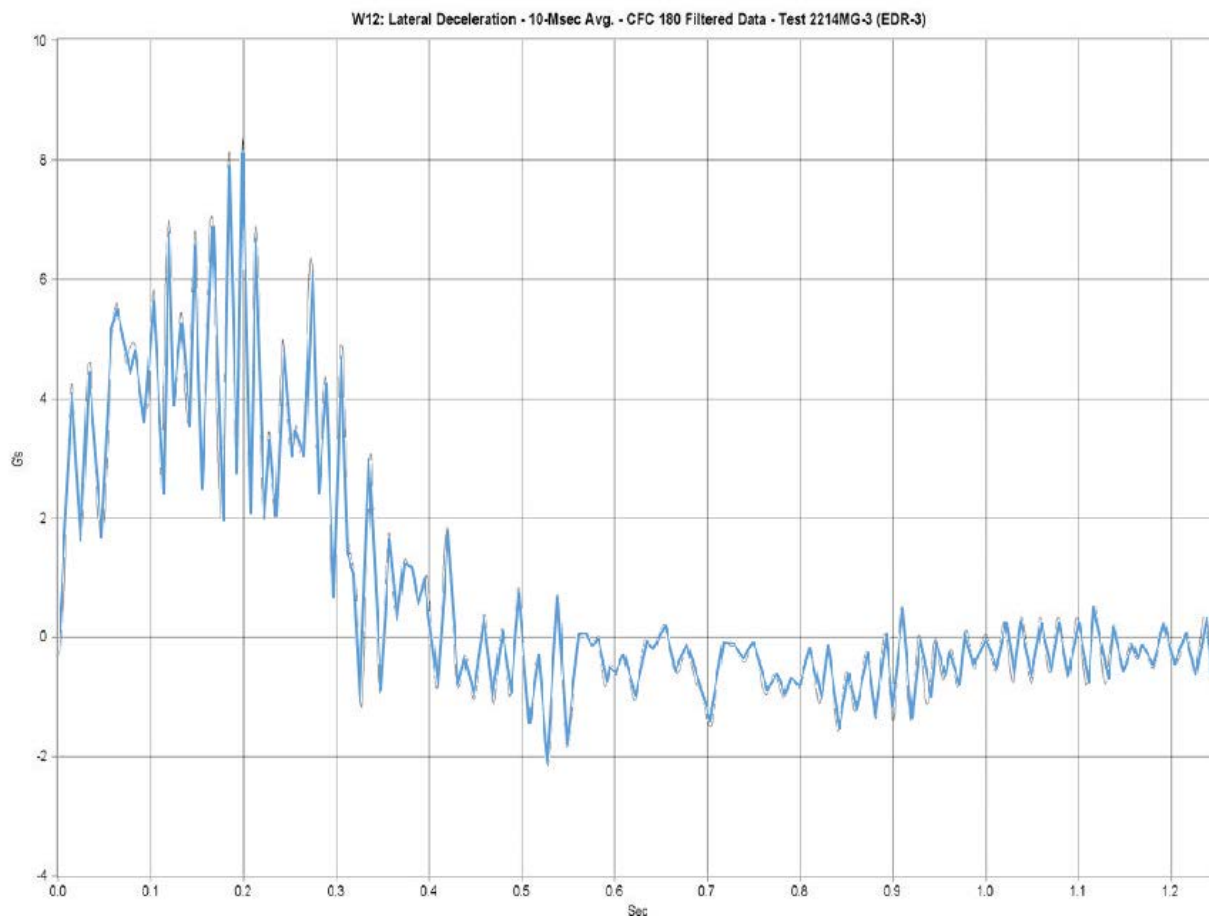


FIGURE 1 Example MATLAB Reading of Crash Test Results

The above referenced method was used to collect maximum longitudinal and lateral decelerations from the identified crash test reports. These reports also provided additional data, including a description of the test article, the mass or weight of the vehicle, its speed and angle at impact, with dynamic and working width of the barrier, and the exit velocity and angle of the vehicle after the redirection. These data are shown in TABLE 1 for a subset of the data pertaining specifically to W-beam guardrail barriers.

TABLE 1 Compiled Data from Test Reports

Test Article		Vehicle			Peak Forces		Widths		Exit	
Type*	Description	Gross Static Weight (lbs)	Speed (mph)	Angle (Deg)	Long. Decel (Gs)	Lat. Decel (Gs)	Dynamic (ft)	Working (ft)	Velo (mph)	Angle
GR	MGS	2,588	60.8	25.4	16.12	8.31	3.00	4.03	30.07	14.10
GR	MGS, Max height	2,599	63.6	25.0	9.15	9.17	2.42	4.12	39.30	12.30
GR	MGS, Max height	2,583	64.1	25.6	11.43	10.89	2.31	3.75	36.20	21.90
GR	MGS, no blockouts	2,578	63.0	25.5	19.28	12.93	2.43	2.88	25.70	19.10
GR	MGS, SYP posts	2,612	61.5	25.3	13.48	14.01	1.85	3.31	35.70	13.60
GR	Modified G4(1S)	5,000	61.1	25.6	19.74	8.40	NA	NA	NA	NA
GR	Modified G4(1S)	5,000	62.4	25.8	9.95	7.21	3.92	4.58	31.19	20.70
GR	MGS	5,000	62.6	25.2	8.93	5.98	3.76	4.78	42.50	7.00
GR	MGS	5,000	62.8	25.5	9.39	6.94	3.65	4.05	39.58	13.50
GR	MGS, long-span	4,991	62.4	24.8	6.93	5.83	7.69	7.79	35.23	1.00
GR	MGS, long-span	4,985	61.9	24.9	7.43	5.60	6.46	7.00	61.91	24.87
GR	MGS, no blockouts	5,181	62.7	24.7	8.25	12.98	2.84	3.60	47.40	14.40
GR	MGS, SYP posts	5,199	62.2	24.9	8.20	8.51	3.33	4.48	37.80	15.70
GR	MGS, Minimum height	5,126	63.1	24.9	9.42	7.90	3.52	4.07	32.90	NA
GR	MGS, mow strip	5,182	63.0	25.2	11.82	7.63	3.53	3.94	34.70	9.70
GR	MGS, omitted post	5,099	63.4	25.3	10.30	7.97	4.08	4.18	27.90	14.00
GR	MGS, downstream anchor	5,172	63.0	26.4	7.49	6.90	32.55	32.55	43.50	4.20
GR	MGS, downstream anchor	2,619	62.0	25.5	20.45	12.07	12.28	12.28	32.20	15.90
GR	Type B	4,484	62.0	27.7	13.09	9.93	3.56	NA	NA	NA
GR	Over curbs	4,482	62.3	28.6	9.25	7.51	3.52	2.37	NA	NA
GR	Low-fill culverts	4,394	64.2	25.3	12.20	11.82	13.64	29.49	39.08	19.50
GR	Low-fill culverts	4,396	62.0	24.8	14.00	14.31	15.51	25.62	42.25	17.30
GR	rock-soil foundations	4,396	61.5	25.4	10.21	7.68	3.21	3.31	37.28	18.00
GR Terminal	SKT-MGS	2,597	64.4	14.5	21.78	9.61	2.31	4.05	43.12	8.80
GR	MGS on 1:2 slope	5,158	61.6	26.3	6.96	5.20	6.08	6.45	40.50	16.00
GR	G4(2W) 8-1/2" PP posts	4,412	60.7	24.8	17.18	24.02	2.40	3.43	25.50	21.30
GR	MGS w/31'3" long span	5,120	62.7	25.3	15.29	5.80	5.13	5.38	27.30	13.30
GR	MGS w/31'3" long span	5,078	61.4	26.3	23.49	10.52	13.68	NA	NA	NA

*GR' = Guardrail

4.3. DETERMINE MINIMUM REDIRECTING FORCE

All tests with a guardrail barrier that resulted in a redirected test vehicle were plotted as shown in FIGURE 2. The x-axis was an index number assigned to the crash test result, but otherwise holds no numerical meaning. Three tests failed to redirect the vehicle, but the reasons were too varied to provide meaningful feedback for this study. As noted in the figure below, the minimum lateral force applied to the vehicle to induce a redirection was 21.5 kips, with an average (neglecting the outlier at index 6) was 36.2 kips.

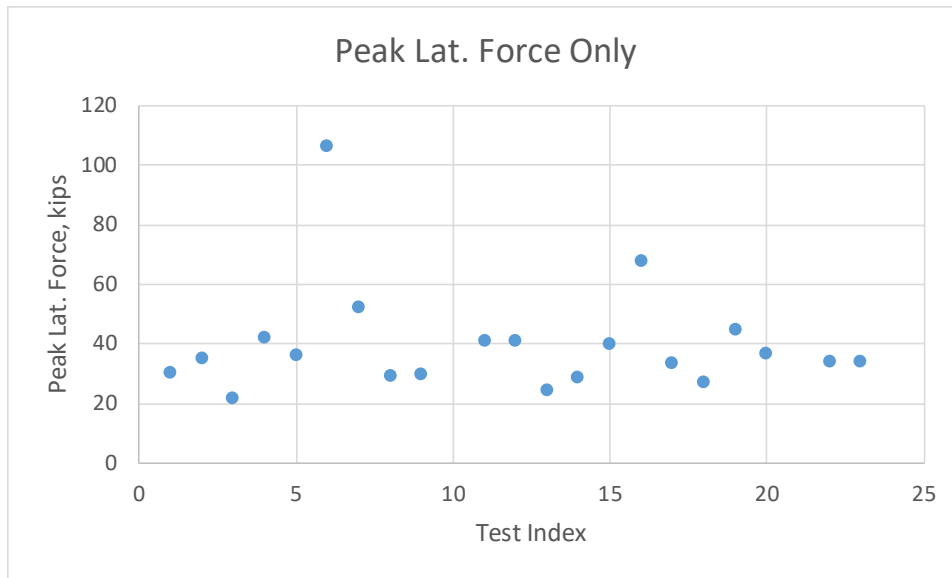


FIGURE 2 Peak Lateral Forces on Redirected Vehicles

4.4. DETERMINE MAXIMUM LATERAL COMPLIANCE

Two considerations were made for lateral compliance: dynamic width and lateral stiffness. Each will be explained in turn. First, dynamic width was plotted for each indexed test, as shown in FIGURE 3. A majority of the results showed a dynamic width between 2 and 5 feet. Some outliers were exceedingly high. However, one non-redirection result was shown (orange dot, index 24), indicating that a barrier that allows too much dynamic deflection simply cannot redirect a vehicle, an observation that should be obvious.

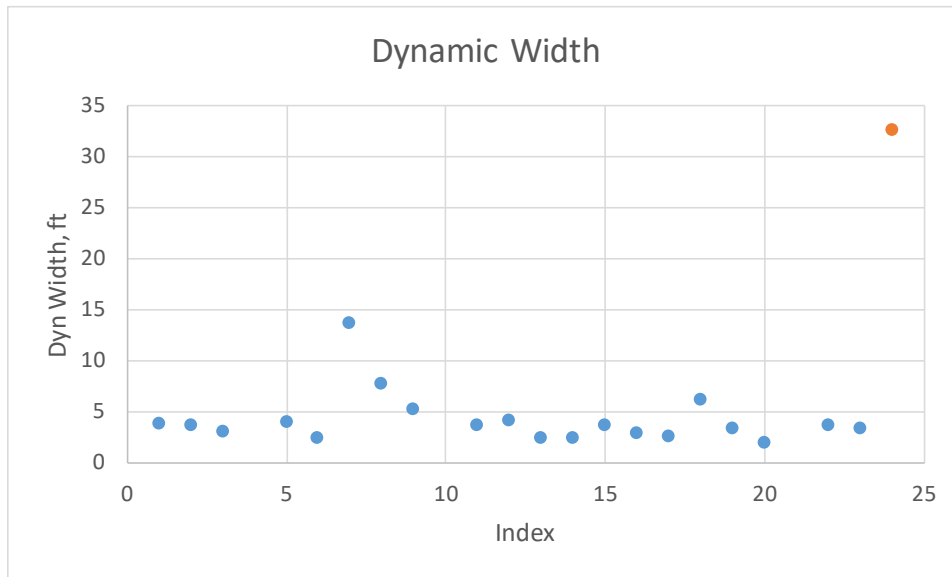


FIGURE 3 Dynamic Width of Guardrail Tests

Second, the dynamic width is part of the combined lateral stiffness. The peak force was divided by the dynamic width to obtain an effective lateral stiffness of the barrier, and the results were plotted as shown in FIGURE 4. The same non-redirection test result (orange dot, index 24) was left in this plot, showing consistency with the previous figure. That is, lateral stiffness of zero allows too much lateral deflection to be effective. Otherwise, the minimum lateral stiffness of guardrail barriers is 3.8 kips/foot with an average of 12.1 kips/foot.

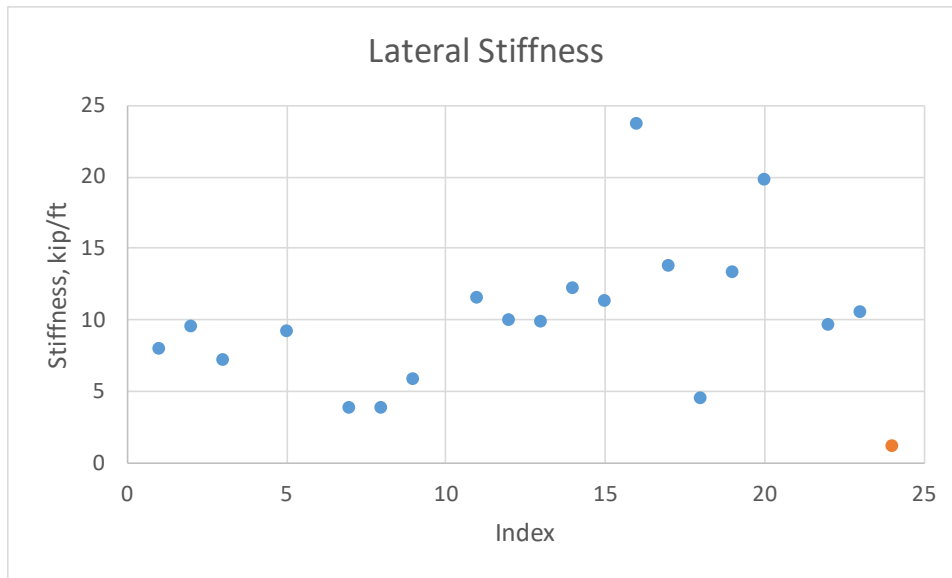


FIGURE 4 Lateral Stiffness of Guardrail Barriers

4.5. CREATE SIMPLE SPRING MODEL IN LS-DYNA

Guardrail terminals have historically been designed with a number of different geometries and energy-absorbing mechanisms. These differences create variations in lateral and longitudinal resistance to displacement. A simple spring model was developed that can replicate these variations implicitly without requiring detailed geometries of the various terminal configurations, including hypothetical configurations that are yet to be developed.

The spring model included a series of rigid plates that interact with the vehicle. These plates can be thought of as the impact plate of terminal. Since these plates exist in space (no posts holding them up), they required boundary conditions in order to replicate real-world applications in terminal design. The plates were allowed to translate in the horizontal plane, but were confined against vertical translation. Also, rotation was permitted about the vertical axis, but not about either horizontal axis.

The springs themselves were attached at one end to the center of the rigid plates. The node at the other end was created in space. One spring was parallel with the theoretical guardrail, and the other spring was perpendicular to the theoretical guardrail. This configuration allowed for the application of a longitudinal and a lateral force, respectively, on the vehicle. Boundary conditions were applied to the node in space for each spring. These boundary conditions allowed the node in space to translate perpendicular to the spring itself. Under these boundary conditions, each spring would apply pure longitudinal or pure lateral forces at all times in the simulation, allowing the research team to easily isolate those forces in post-processing.

Two different spring models were developed and used for two impact locations in this analysis: (1) corner; and (2) the front-bumper quarter point. The corner impact spring model was built out of rigid shells oriented at a 90-degree angle, as shown on the left in FIGURE 5. In contrast, the quarter-point model was more like a common impact plate for existing terminal designs. It was narrow with vertical “teeth” designed to engage the vehicle. This model is shown on the right in FIGURE 5. It is also important to note that the results of this analysis depend on the connection between the vehicle and the terminal remaining intact throughout the crash.

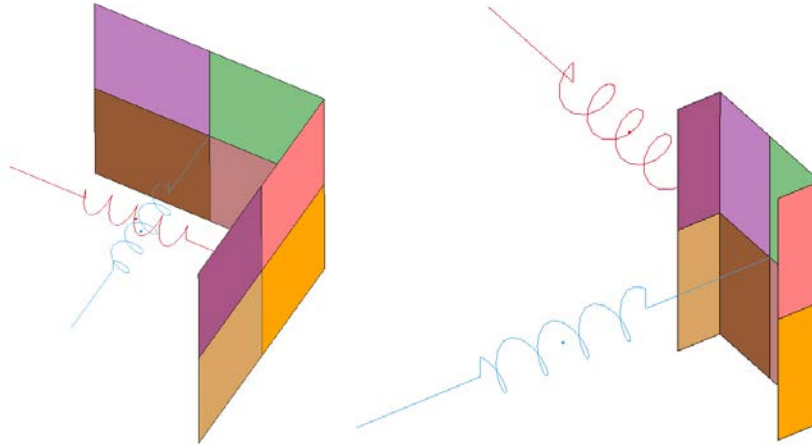


FIGURE 5 Isometric View of Spring Model

4.6. DEBUG THE LS-DYNA SPRING/TRUCK MODEL

A full-scale Silverado pickup truck was used as the subject vehicle in the LS-DYNA simulations. This vehicle model was developed by the National Crash Analysis Center at the George Washington University. It was based on a 2007 Chevrolet Silverado. This vehicle is a typical representative of the MASH 2270P vehicle. Since this vehicle represents the maximum loading from the test matrix in MASH, it was the only vehicle used in these simulations. The spring model was oriented around the vehicle to replicate a 15-degree impact. An overhead view of a corner impact (left) and quarter point impact (right) is shown in FIGURE 6. As with most models, there were some complications with regard to running these simulations. Contact between the rigid plates and the vehicle was attempted by multiple algorithms. Eventually, the part numbers were simply added to the list of vehicle parts whose contact was controlled by `*CONTACT_ AUTOMATIC_SINGLE_SURFACE`. In addition, the boundary conditions described in the previous section were finalized by investigation in this task.

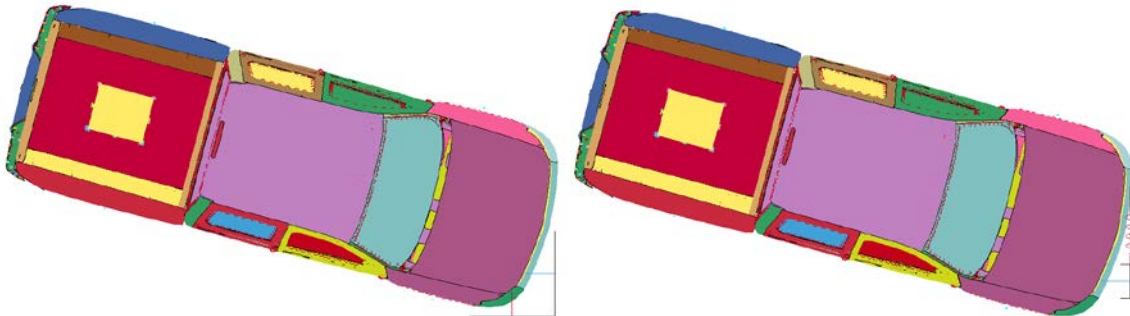


FIGURE 6 Overhead View of the Truck and Spring Model

4.7. TUNING THE SPRING STIFFNESS

Due to the fact that numerous concepts currently exist in the terminal market, it was determined that a range of applicable lateral and longitudinal forces would provide the freedom for this disparity to continue. Also, when designing a terminal, the designer needs to be aware of the quantitative effect of the stiffness variables in order to properly design a non-gating terminal. As such, the stiffnesses of the two springs were altered in numerous ways to investigate their effect on the trajectory of the vehicle. Each spring was defined by two parameters, the modulus in the elastic zone and the yield force. To create this effect, the `*MAT_SPRING_ELASTOPLASTIC` material model was selected. Referring to FIGURE 7, the modulus was represented by “k” and the force was represented by “Fy”. This material model was selected because it reflects the reality of guardrail systems generally. For small deflections (note that the material model shown in FIGURE 7 is not a scale model), guardrail systems have an elastic response. That elastic response is greater in the lateral direction, meaning

“k” in the lateral direction must be small to flatten the curve and extend the elastic region. In contrast, terminal forces in the longitudinal direction ramp up to their constant force very quickly, making the longitudinal elastic stiffness quite large.

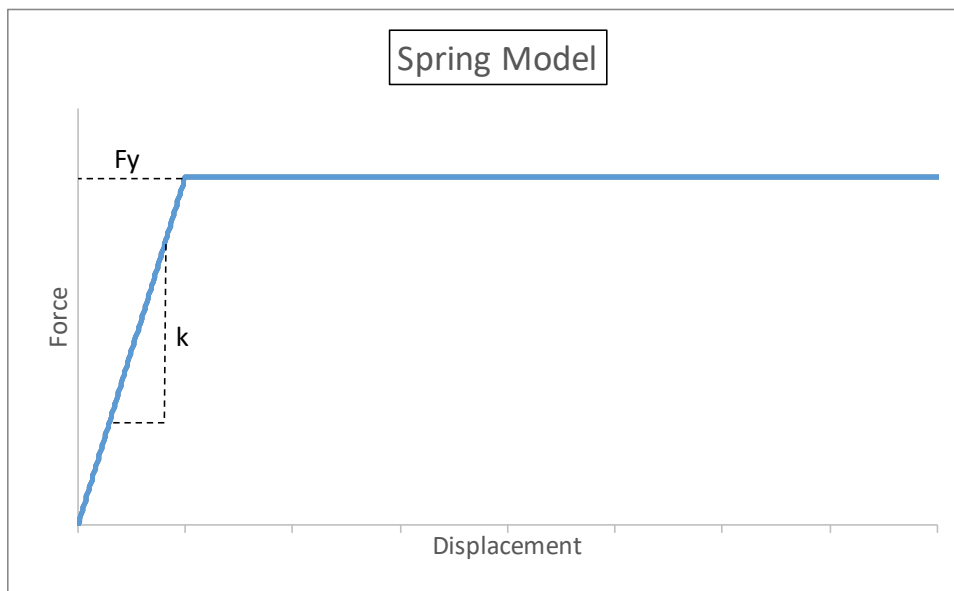


FIGURE 7 Elastic-Perfectly Plastic Spring Model

4.7.1. Single-Variable Parametric Study - Corner Impacts

With two springs, there were four different parameters to modify. Each one was simulated with five different values, which are shown in TABLE 2. The middle values, highlighted in yellow, were the baseline model. When one variable was being analyzed, the other three were set to this baseline value. This process was done for a corner impact using the spring model described previously, resulting in 25 separate models. A description of the direction for the applied spring forces, relative to the vehicle, is shown in FIGURE 8. The baseline model from the first series was reused in post-processing to reduce the number of simulations by three. Results from these 25 simulations are shown in TABLE 3.

TABLE 2 Values used in Parametric Study

k1 (N/mm)	k2 (N/mm)	Fy1 (N)	Fy2 (N)
1,000	50,000	47,820	22,500
2,000	75,000	71,730	33,750
3,000	100,000	95,640	45,000
4,000	125,000	119,550	56,250
5,000	150,000	143,460	78,750

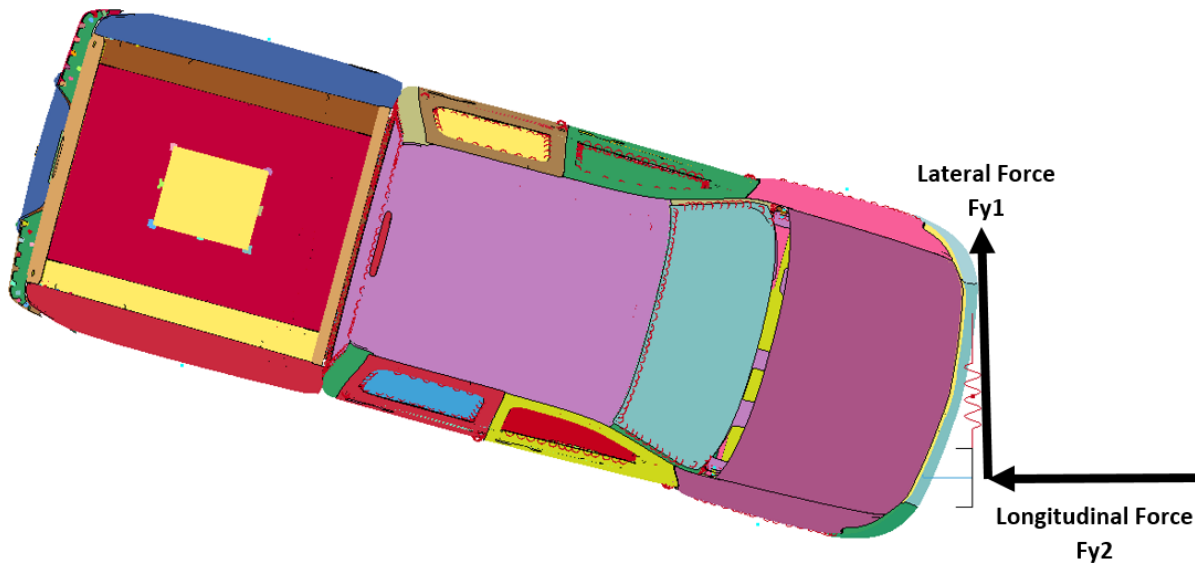


FIGURE 8 Description of Force Directions Relative to the Vehicle

TABLE 3 Single-Variable Parameter Study Results

	Run	k1 (N/mm)	k2 (N/mm)	Fy1 (N)	Fy2 (N)	Description	Peak y-displ (mm)	Veh a_x (g's)	Veh a_y (g's)
k1	1	1000	100000	95640	45000	Redirected	302	-5.34981	6.79239
	2	2000	100000	95640	45000	Redirected	267.5	-5.34981	7.58642
	BASELINE	3000	100000	95640	45000	Redirected	260.4	-5.55554	7.29868
	4	4000	100000	95640	45000	Redirected	255.4	-5.34981	7.66565
	5	5000	100000	95640	45000	Redirected	250.928	-5.34981	7.77898
k2	6	3000	50000	95640	45000	Redirected	258.651	-5.65748	7.30928
	7	3000	75000	95640	45000	Redirected	259.583	-5.40264	7.87781
	BASELINE	3000	100000	95640	45000	Redirected	260.4	-5.55554	7.29868
	8	3000	125000	95640	45000	Redirected	259.914	-5.34981	7.35474
	9	3000	150000	95640	45000	Redirected	260.582	-5.34981	7.38532
fy1	10	3000	100000	47820	45000	Redirected	773.535	-5.34981	4.8625
	11	3000	100000	71730	45000	Redirected	399.932	-5.34981	5.91692
	BASELINE	3000	100000	95640	45000	Redirected	260.4	-5.55554	7.29868
	12	3000	100000	119550	45000	Redirected	179.987	-5.34981	9.19113
	13	3000	100000	143460	45000	Redirected	106.44	-5.39994	10.3314
fy2	14	3000	100000	95640	22500	Redirected	221.768	-4.9464	10.0551
	15	3000	100000	95640	33750	Redirected	232.296	-4.68909	9.31696
	BASELINE	3000	100000	95640	45000	Redirected	260.4	-5.55554	7.29868
	16	3000	100000	95640	56250	Redirected	274.99	-5.85932	7.89973
	17	3000	100000	95640	78750	Redirected	312.97	-7.4451	7.33475
k1	18	1	100000	95640	45000	Gated	4395.33	-4.94221	-3.28542
	19	10000000	100000	95640	45000	Redirected	235.951	-5.34981	9.57156
k2	20	3000	1	95640	45000	Redirected	231.938	-3.61876	7.80954
	21	3000	10000000	95640	45000	Redirected	260.442	-5.40076	7.70642
fy1	22	3000	100000	1	45000	Gated	4727.72	-4.94221	-3.31957
	23	3000	100000	10000000	45000	Redirected	61.2022	-5.96032	10.7597
fy2	24	3000	100000	95640	1	Redirected	231.097	-3.72069	7.52935
	25	3000	100000	95640	10000000	Crushed	NA	NA	NA

Using these results, the effect of each variable on key outcomes, such as peak displacement in the y-direction and accelerations in the x- and y-directions, was investigated. Individual plots were created, and a curve was fit to each set of results. Using a simple regression tool, R^2 , the closeness of the fit for each plot was reviewed to determine if there was a clear effect of the subject variable on the dynamics of the vehicle. Based on these plots and curve-fits, which are provided in Appendix A, an interpretation of the results was performed where the fit was judged on a scale of 1 (no effect) to 5 (extreme effect). The results of this interpretation are shown in FIGURE 9. The main correlation was between the overall applied forces, $fy1$ and $fy2$, and the peak y-displacement. These variables were considered further in the two-variable parametric study described in the next subsection. There were two other outcomes that demonstrated a close fit: $k1$ and $fy1$ on the results of y-acceleration of the vehicle. However, closer examination of these plots, Figure A1 and Figure A3 in Appendix A, shows that for these variables, the curve is highly logarithmic. While that is not enough to be concerned about alone, the nature of the curves was clearly controlled by a single test result. As such, it was not considered a reliable outcome. In addition, the acceleration of the vehicle came to be seen as less vital than the peak y-displacement in the determination of gating versus non-gating. Larger deflections create larger strains, and by extension, stresses. This leads to the formation of a plastic hinge, after which the gating action follows.

	Peak Y	a_x	a_y	
k1	3	1	4	1 none
k2	1	2	1	2 slight
fy1	5	1	4	3 moderate
fy2	4	2	2	4 significant
				5 extreme

FIGURE 9 Interpretation of Single-Variable Parametric Study

4.7.2. Two-Variable Parametric Study – Quarter-Point Impacts

Next, due to the observation that the constant forces were more predominant than the elastic moduli, a two-variable parametric analysis was performed. This allowed the research team to investigate the various combinations of the two forces directly, rather than needing to extrapolate from the single-variable parametric study. For each value of “ $Fy1$ ”, the other parameter, “ $Fy2$ ” had five values, making in total 25 simulations, as represented by the diagram in FIGURE 10. Units in this diagram are in Newtons.

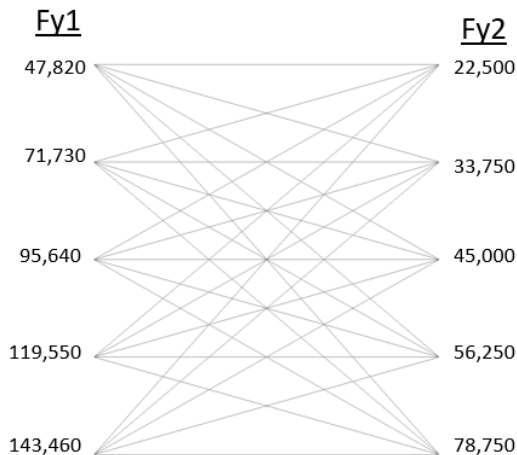


FIGURE 10 Two-Variable Parametric Study

As with the single-variable approach, a 5,000-lb Chevrolet Silverado model was used in the LS-Dyna simulations. The resultant velocity vector of the accelerometer element in the vehicle was used to calculate the velocity in the x- and y-direction, relative to the barrier. To do so, the velocity of the vehicle had to be rotated by the initial angle of 15 degrees using the two equations below:

$$V_x = V'_x \cos \theta - V'_y \sin \theta$$

$$V_y = V'_x \sin \theta + V'_y \cos \theta$$

Where: V_x is the velocity of the vehicle in the direction parallel with the barrier
 V_y is the velocity of the vehicle in the direction perpendicular with the barrier
 V'_x is the velocity of the vehicle in the heading direction of the vehicle
 V'_y is the velocity of the vehicle perpendicular to the heading direction of the vehicle
 θ is the initial angle of the vehicle relative to the barrier

The vehicle was considered to be redirected when the velocity component perpendicular to the barrier (V_y) reached zero. In contrast, with a non-zero velocity in the perpendicular direction, the vehicle would pass behind the barrier, fulfilling the basic definition of a gating event. As noted above, five different stiffnesses were analyzed for both lateral and longitudinal loads. The results are shown in FIGURE 11. In this figure, each plot relates to a specific lateral load. The x-axis was the ratio of the longitudinal load to the given lateral load. For example, when the lateral load was 47,820 Newtons (11 kips) and the longitudinal load was 22,500 Newtons (5.06 kips), the ratio of longitudinal to lateral was 0.47. For each given lateral load, this ratio was plotted against the calculated velocity component that was perpendicular to the barrier. As can be seen from these plots, it was not possible to fully redirect the vehicle for a lateral load of 11 kips, regardless of the longitudinal load. However, for the remaining lateral loads, a redirection envelope was observed. A trend line was fit through the upper and lower bounds, both of which exhibited high R^2 values. Setting “y” equal to zero and solving both equations produced a range of ratios and lateral loads that define this envelope. For a lateral load of 32 kips, zero y-velocity was reached at a ratio of 0.75. For a lateral load of 16 kips, zero y-velocity was reached at a ratio of 1.5. Results are tabulated in Appendix B. Therefore, given a minimum of 16 kips for a lateral load, redirection is possible under the following criteria:

$$F_{lat} \geq 16 \text{ kips}$$

AND

$$(0.75 \times F_{long}) \leq F_{lat} \leq (1.5 \times F_{long})$$

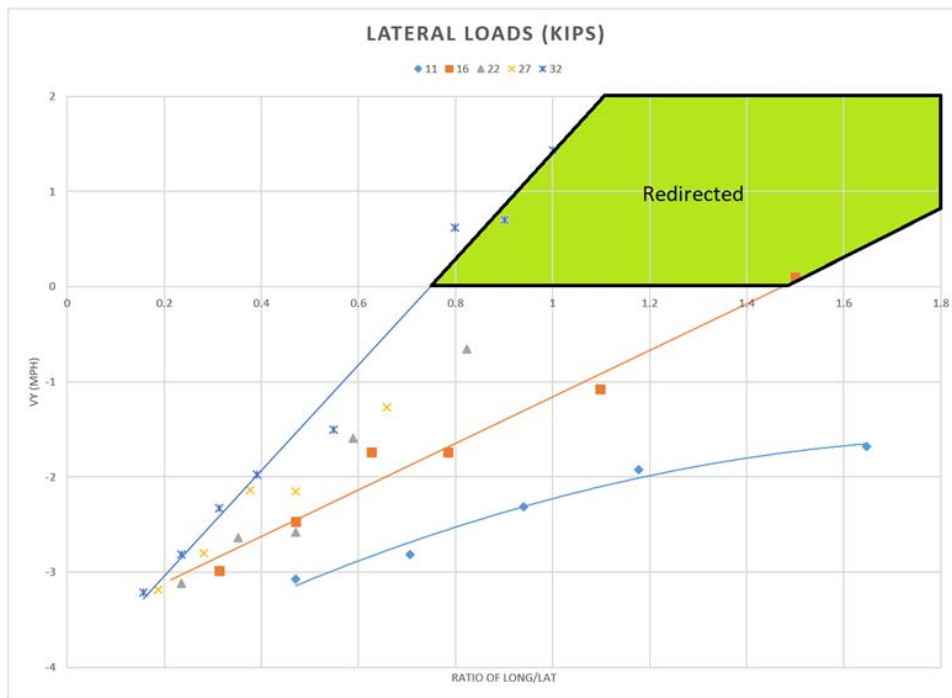


FIGURE 11 Results of Lateral and Longitudinal Loading on Redirection Results

4.8. FULL-SCALE SIMULATIONS

The previous section described an analysis that applies generally to any external set of forces being applied to a vehicle. Full-scale simulations described in this section deal more closely with real-world W-beam barrier designs. Specifically, a 12-gauge W-beam rail was suspended from posts via post bolts and blockouts, similar to an actual W-beam strong-post guardrail system. However, in order to adjust the lateral force exerted on the vehicle by the barrier, the posts were not standard line posts. Instead, square tube posts, with a slot in the back, were chosen, as shown in FIGURE 12. In each subsequent model, the cross-section was modified, which altered the post's critical plastic moment. In effect, this was a real-world interpretation of the lateral load discussed in the previous section.

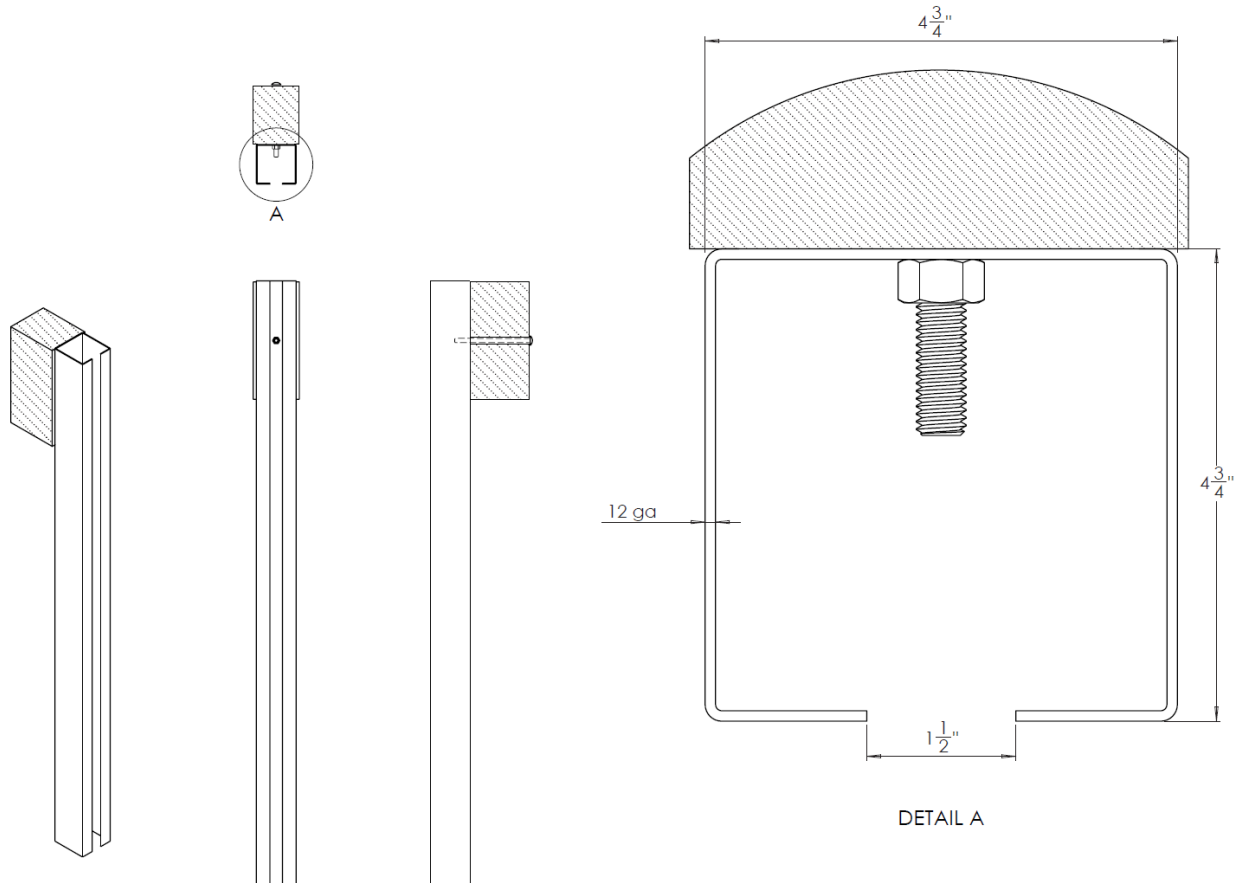


FIGURE 12 Example of Post Geometry

Next, energy-absorbing guardrail terminal heads have their own inherent rate of energy absorption. This rate translates to an average longitudinal force for that terminal. In the present analysis, the research team modeled a new tension-based energy-absorbing guardrail terminal, currently under development for another project. This terminal head is constructed with a series of internal plates and wedges that fold the guardrail in half, thus absorbing energy. The rate of this absorption is easily modified by changing the position and size of the plates and wedges in the terminal head. Therefore, making modifications to the geometry of this folding-type guardrail terminal head became the real-world interpretation of the longitudinal load discussed in the previous section. Multiple versions of the folding-type guardrail terminal were considered using the non-linear finite element code LS-Dyna. As an example, four versions which were considered using LS-Dyna wherein the feeder chute, the length of the folding region, and the overall width of the impact plate were modified are shown schematically in Appendix C.

The results of an extensive analysis of post designs using the Version 3 design shown in FIGURE C1 are shown in FIGURE 13. In this study the forces were increased by modifying the coefficient of friction acting between the guardrail

terminal head and the W-beam guardrail. An increase in the coefficient of friction results in an increase in the longitudinal (head-on) and lateral forces. LS-Dyna uses three parameters in order to determine the coefficient of friction acting on the system: (1) the static friction coefficient (FS), (2) the dynamic friction coefficient (FD), and (3) an exponential decay coefficient (DC). The contact friction value, μ_c , is determined using the function below.

$$\mu_c = FD + (FS - FD)e^{-DC|v_{rel}|}$$

Here v_{rel} is the relative velocity of the contacting surfaces. When v_{rel} is high the dynamic friction coefficient will dominate, however as v_{rel} approaches zero the static friction coefficient will take over. The rate of the transition from FD to FS is governed by the exponential decay coefficient. As can be seen from the equation, when $FS = FD$ the second term cancels and the value for DC is irrelevant. In finite element modeling friction is highly mesh dependent due to piecewise linear contours of the meshed geometry making the surface artificially rough and therefore values for FS, FD, and DC cannot be determined using empirical measures. As a result a calibration study was conducted to determine the values for FS, FD, and DC that provided the best approximation to experimental results. This study showed that values of $FS=0.4$, $FD=0.02$, and $DC=0.0004$ gave the best fit to experimental results for a range of impact conditions. This set of coefficients are indicated by the circles in FIGURE 13. Other friction values were used to approximate other terminal head geometries which result in higher or lower longitudinal and lateral forces. In this study the crosses represent $FS = FD = 0$, triangles represent $FS = FD = 0.1$, diamonds represent $FS = FD = 0.2$, and squares represent $FS = FD = 0.3$.

For each friction coefficient, eight different post geometries were analyzed to study the effect on the vehicle. Each point on the graph represents a combination of three tests from MASH which utilize the 5000 lb pickup truck: 3-31, 3-33, and 3-35. Test 3-31 was used to establish the value for the head-on force, while 3-33 and 3-35 were used to examine gating and redirection respectively. If a combination of head-on force and plastic moment resulted in a failure of any of these tests based on MASH criteria then the combination was considered inadmissible and is represented with a red symbol. If all tests passed then a green symbol was used. In all cases, test 3-31 produced acceptable results, and test 3-33 was the critical test for determining performance. Furthermore, in cases where the plastic moment was below 8,000 ft-lb the posts did not provide adequate stiffness for test 3-35 to prevent the vehicle from overriding the system, however, in these cases the vehicle either gated or rolled over in test 3-33 as well. By interpretation, the research team has concluded that any combination of head-on force and plastic moment of the post that falls in the green shade region of FIGURE 13 will result in a successful non-gating event.

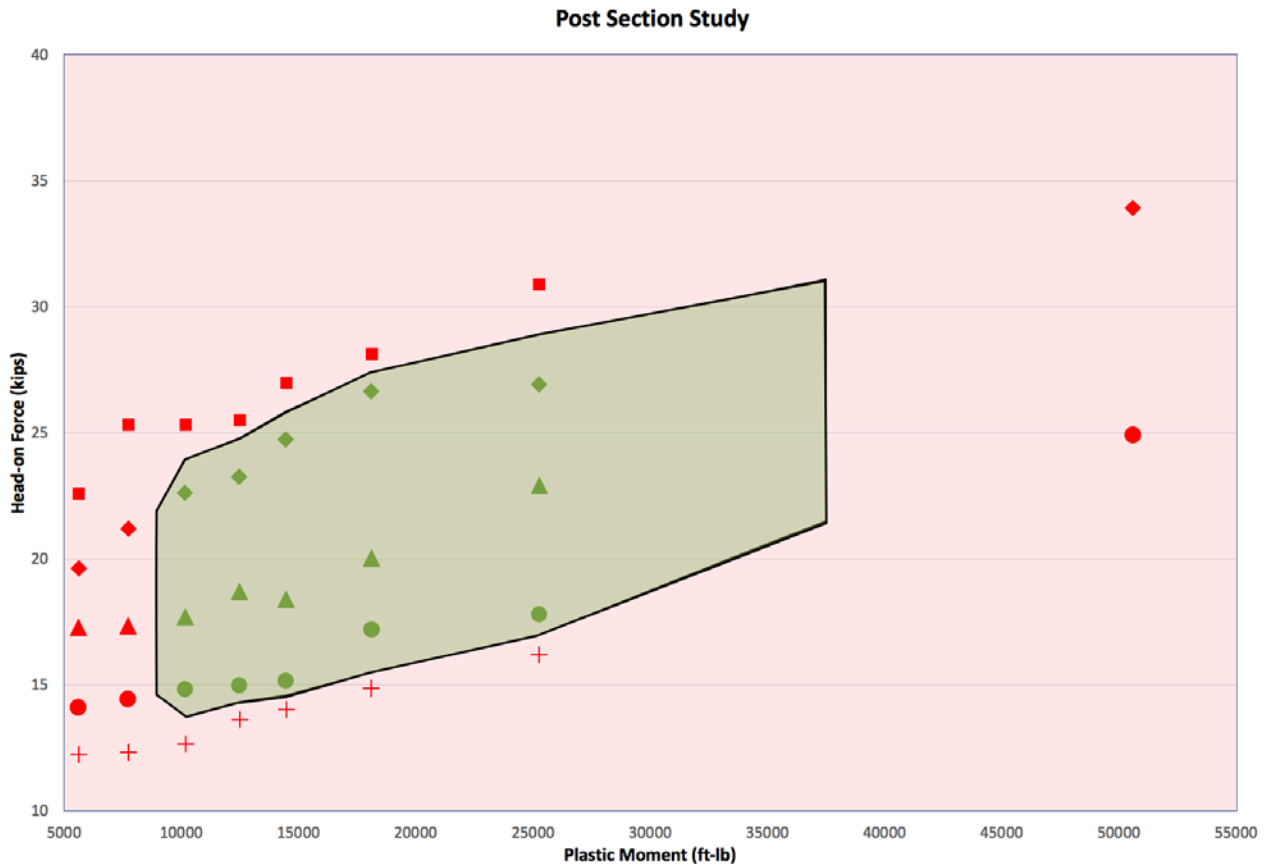


FIGURE 13 Results of Post Section Study

4.9. BRAINSTORMING PROTOTYPE CONFIGURATIONS

The research team met often to discuss ideas for creating a physical prototype capable of generating the lateral and longitudinal forces identified in Stage 2. The ideas fell into one of three main categories: (1) creating an all-new system; (2) retrofitting an existing system; and (3) converting a terminal already under development into a non-gating system.

The leading candidate for an all-new system was an extruding-type terminal that also had a cable running the length of the system. The cable would be anchored to the guardrail at about the 50-ft mark and attached to the guardrail intermittently using U-bolts or J-bolts, which would easily shear off. The cable would feed through the terminal head, and just prior to the guardrail undergoing the extrusion process, the cable would split off and exit a small hole in the bottom of the terminal head. During the analysis of this design concept, it was observed that the terminal was a hybrid between tension-based and compression-based systems. The guardrail was almost entirely in compression, and the cable provided tension only for redirection-style impacts. This led to some instabilities for high-energy impacts. It was also discovered that the interaction of the cable and the terminal head was too dependent on the clearance between the terminal head and the guardrail itself. If the guardrail buckled from the compressive load, there was a risk that there would be too little clearance for the terminal head to continue. Finally, the cable itself was in a compromised position, with the possibility that it could rub on the edges of the terminal and fail to maintain membrane action throughout the impact.

The second category involved connecting a cable directly to the guardrail of an existing product. The basic idea shared by these brainstorm ideas was that the first panel of guardrail used in the compression-based system would be rigidly connected to a cable, which in turn would be anchored to the ground and not able to release in an end-on impact. However, this approach was abandoned upon realizing that the different systems would each require a unique design. Also, some of them would make it impossible to create a strong enough connection between the cable and the guardrail. Finally, they also exit guardrail to the side. This would place the extruded guardrail and cable in the path of the vehicle, which could lead to rollover or a connection failure.

The research team settled on a converting an emerging technology into a non-gating system. This new terminal was under development by the research team as part of another project. It formed the basis for the full-scale modeling done in Stage 2 of this project. Therefore, it was already known that the longitudinal forces could be tuned as needed to match the lateral forces. From there, square posts were modified based on a review of existing literature and a similar project done by the research team. This similar project was an attempt to create new guardrail posts that softened the system longitudinally but maintained strength laterally. Using these two previous projects helped expedite this project and resulted in a quick turnaround for fabrication.

The folding terminal head is built of 10- and 12-gauge steel. Many of the parts are laser cut before being bent and assembled. Based off of the full-scale modeling, the dimensions of the parts necessary to produce an optimal longitudinal force were drawn and sent to a laser cutter. The pieces were assembled at the research team's fabrication shop. The parts were welded together and sent to a galvanizer to produce the prototype terminal head.

Posts were also built at the research team's fabrication shop. They were constructed from 12-gauge steel and bent into channels. Then, two channels were welded together to produce a square post with an opening on the backside, making it an open, thin-walled cross-section.

The first panel of W-beam was modified to attach a short cable. The cable had a swaged button on the end which was set into a rectangular hole cut out of the W-beam valley, near the end. Additional plates of 12-gauge were mounted around the button to strengthen the connection and prevent crack propagation. Finally, model results showed some high plastic strains in the valley of the W-beam near the post bolt holes. Therefore, the prototype included some additional 12-gauge plates around these holes to arrest any cracks that might develop.

Finally, the cable was anchored to a large steel post. The ground-side end of the cable had a threaded fitting swaged onto it, and the fitting was rigidly attached to a gusseted bracket. This bracket was securely welded to a plate, which in turn was welded to the end of a W8X15 steel post. This post also included a soil plate. The whole assemble was driven into soil. The terminal head was slid over the W-beam with the cable being fed through the folding mechanism and out of the bottom of the head. It was then connected to the anchor post, and the cable was tightened as any cable anchor would be for a guardrail terminal.

4.10. CRASH TEST EVALUATIONS OF PROTOTYPE

The outdoor lab used by the research team includes a 300-ft concrete pad, with an additional 300-ft runway. At the end of this run, the prototype guardrail terminal was installed at 15 degrees relative to the line of the runway. The layout of the system was such that the terminal head would impact the center line of the front of the test vehicle.

A 60-ft by 30-ft cutout was removed from the concrete where the square posts would be installed. At the end of the 50-ft length of terminal guardrail, the posts reverted back to standard line posts, and rather than be driven into soil, they were bolted to the concrete (with the length shortened). The downstream end was anchored to the concrete with two opposite-direction BCT cable anchors.

The galvanized terminal head was slid over the guardrail, and the cable was fed through the head. Then, the cable was bolted to the anchor post, which with its soil plate, had been driven into the soil. A photo of the test configuration is shown in FIGURE 14.



FIGURE 14 Test setup (left) without terminal head and (right) with terminal head







Previous development efforts related to the folding terminal demonstrated that a bogey vehicle is a strong surrogate for frontal, zero-degree, center-line impacts. However, when considering angled impacts, the bogey vehicle is woefully inadequate. It has a rigid frame and cannot steer. This means that the energy absorbed by the crush of a normal vehicle must now be absorbed during an oblique hit. In addition, for a non-gating terminal to function, it must steer the vehicle back to some degree. The rigidity of the frame for the bogey vehicle prevents this.

It was important to evaluate the prototype with a real vehicle. As part of the previous work done to develop the folding terminal, a local salvage yard was inspected for adequate vehicles. The research team found several Ford Explorers that rolled straight. A deal was arranged with the salvage yard to transport vehicles to the test lab and pick them up again after the crash test.

For the present design, two tests were conducted, one with a Ford Explorer and one with a Mazda Protégé. While these tests were based on MASH test guidelines, they were not compliance tests and, as such, were strictly investigative evaluations. The primary difference was that the Ford Explorer weighed less than the MASH test vehicle, and its speed was less than required. Also, no crash test dummy was used in the Mazda Protégé test. In both tests, the age of the vehicle was older than recommended by MASH. Details of the impact conditions for each test are provided in the preceding paragraphs.

The first test involved a Ford Explorer, which weighed approximately 4,200 pounds. The speed at impact was 49.8 mph, based on the results of integrating the accelerometer data. The calculated Occupant Ridedown Acceleration (ORA) was 9.6 Gs, while the Occupant Impact Velocity (OIV) was only 22.6 ft/s, both of which are well below the limit specified in MASH. The vehicle traveled nearly 22 feet before spinning out to the backside of the barrier. However, unlike any other terminal before it, the vehicle's forward progress had been completely stopped. In other words, the vehicle did not continue on to the backside of the barrier. Sequential images of this test are provided in TABLE 4. In addition, the force-deflection data from the accelerometer mounted to the vehicle is shown in FIGURE 15. This data was collected at 10,000 Hz by a DTS Slice accelerometer.

TABLE 4 Sequential Images of the Ford Explorer Test

Time (msec)	Ford Explorer
0	 <p>A top-down view of a dark-colored Ford Explorer SUV on a concrete test track. The vehicle is positioned at the start of a curved barrier. A mechanical arm is visible on the left side of the frame.</p>
120	 <p>The Ford Explorer is shown in the middle of the curve, with the barrier beginning to deform and pull away from the vehicle.</p>
240	 <p>The vehicle is now partially inside the barrier, which is significantly crumpled. Debris is scattered on the ground around the car.</p>
360	 <p>The Ford Explorer is almost completely surrounded by the collapsed barrier. The impact has caused significant structural damage to the vehicle's side.</p>
480	 <p>The vehicle is now mostly free from the barrier, which has been pushed back and is in a state of total collapse. The car appears to be in a state of motion.</p>
600	 <p>The Ford Explorer is shown moving away from the barrier area, having successfully navigated the obstacle. The barrier remains in its collapsed state.</p>

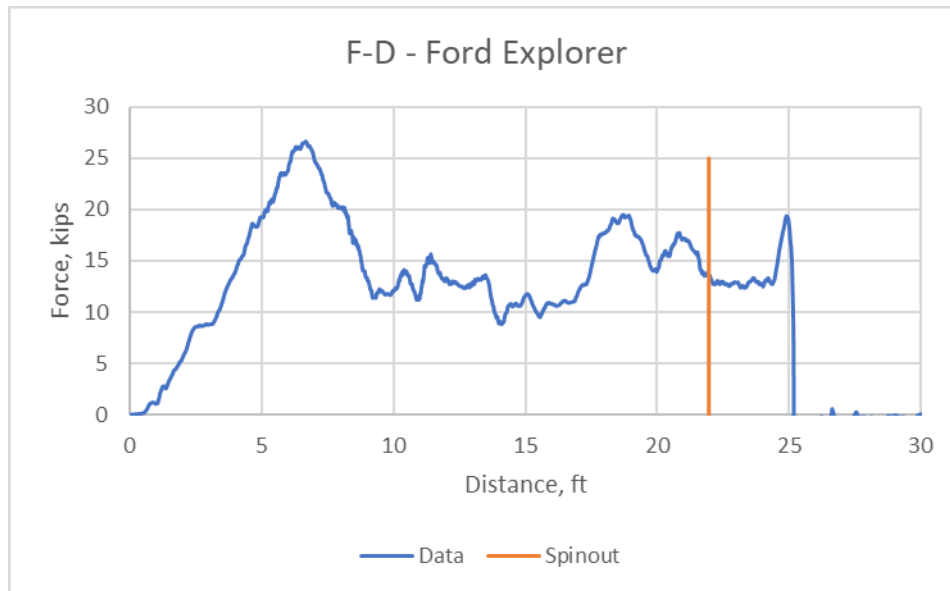







FIGURE 15 Force-Deflection Curve for Ford Explorer at 15 Degrees

The second test involved a Mazda Protégé, which weighed approximately 2,493 pounds. The speed at impact was 64.1 mph, based on the results of integrating the accelerometer data. The calculated ORA was 12.8 Gs, while the OIV was only 33.1 ft/s, both of which are well below the limit specified in MASH. The vehicle traveled nearly 20 feet before spinning out to the backside of the barrier. However, unlike any other terminal before it, and similar to the Explorer test, the vehicle’s forward progress had been completely stopped. In other words, the vehicle did not continue on to the backside of the barrier. Sequential images of this test are provided in TABLE 5. In addition, the force-deflection data from the accelerometer mounted to the vehicle is shown in FIGURE 16. This data was collected at 10,000 Hz by a DTS Slice accelerometer.

TABLE 5 Sequential Images of the Mazda Protégé Test

Time (msec)	Mazda Protégé
0	 <p>A photograph of a silver Mazda Protégé sedan at the start of a test. The car is positioned on a dark asphalt surface, facing a metal barrier. To the left of the car is a green metal structure. The background is a light-colored concrete or asphalt area.</p>
120	 <p>A photograph showing the Mazda Protégé beginning to rotate and lean towards the barrier. The car's front end is closer to the barrier, and its body is angled.</p>
240	 <p>A photograph where the Mazda Protégé is leaning significantly towards the barrier. The car's front is in contact with the barrier, and its rear is still on the asphalt.</p>
360	 <p>A photograph showing the Mazda Protégé leaning further towards the barrier. The car's front is more deeply engaged with the barrier, and the rear is starting to lift slightly.</p>
480	 <p>A photograph where the Mazda Protégé is leaning almost vertically towards the barrier. The car's front is heavily impacted, and its rear is high in the air, indicating a near-overturn.</p>

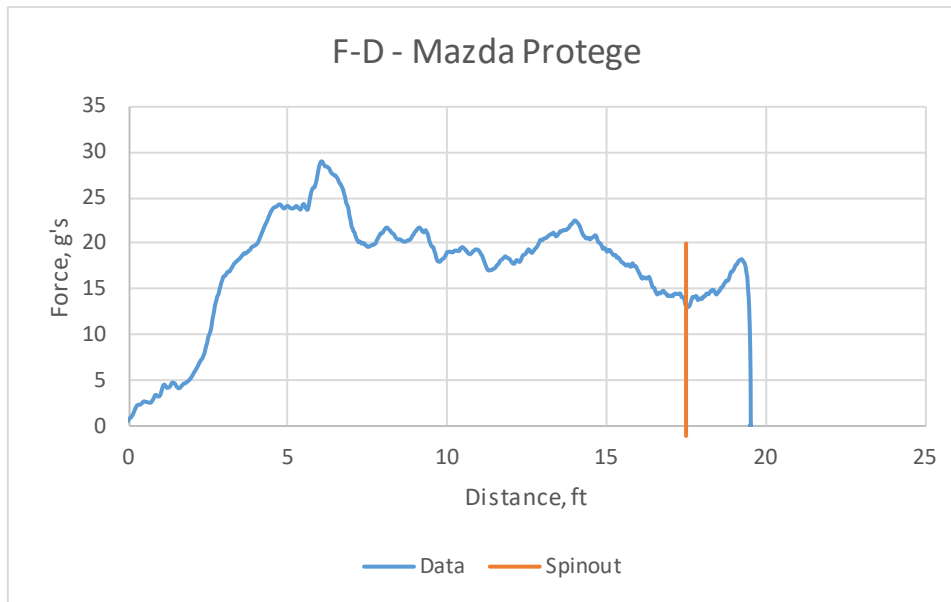


FIGURE 16 Force-Deflection Curve for Mazda Protégé at 15 Degrees

5. CONCLUSIONS

Before now, gating was a feature of all guardrail terminals, and such behavior was taken for granted. Design policies have reflected this inherent characteristic by requiring long run-out lengths, which permit gating far enough away from the shielded hazard. However, this project has proven that a non-gating guardrail terminal is possible, and that essentially non-gating performance has already been achieved with the first prototype.

During the development, various aspects were investigated that were originally deemed relevant to the non-gating event. First, non-gating is a natural feature of guardrail within its length-of-need. Therefore, crash tests on guardrail were investigated to understand how much lateral and longitudinal force they imparted on the vehicle as well as how much lateral deflection they permitted. As a first step, this literature review and analysis was helpful in forming an understanding of redirection, but it became clear that redirection is not the primary factor in determining if a terminal with gate or not. A length-of-need portion of guardrail benefits from an upstream and a downstream length of guardrail pulling on the vehicle to change its heading. A terminal only has the downstream portion, making it much weaker. Therefore, it became clear that some surrogate was required to imitate the upstream length of guardrail. To do so, a cable was rigidly attached to the guardrail and bolted to an anchor post at the ground level. This also, effectively, created a tension-based system.

It was also learned as part of this investigation that the lateral and longitudinal forces must be considered together in designing a non-gating terminal. In other words, for a given lateral force, there is a range of longitudinal forces that will satisfy the non-gating requirement. Longitudinal forces above or below that range will result in gating. The same is true in reverse, for a given longitudinal force, lateral forces are confined to a range.

Using these understanding, and the tools developed through simulation, a prototype was designed, constructed, and tested at the research team’s test lab. The prototype was constructed at a 15-degree angle with respect to the vehicle trajectory. Two tests were conducted: (1) a Ford Explorer at 50 mph; and (2) a Mazda Protégé at 64 mph. In both crashes, a significant amount of rail was fed through the terminal head, which led to a full stop of the vehicle’s forward velocity. The vehicle never passed behind the terminal head, making it possibly the first terminal to do so.

6. PLANS FOR IMPLEMENTATION

A prototype was developed as part of this project to prove the concept of a non-gating guardrail terminal that meets the criteria for longitudinal and lateral forces, as outlined herein. That prototype has been successfully crash tested using common vehicle types. From this point forward, the prototype terminal will continue to be developed and prepared for full-

scale crash testing according to the MASH protocol for non-gating guardrail terminals. This will likely include a full battery of tests including zero-degree head-on impacts, 15-degree impacts on the end, and reverse direction impacts. When complete, a pilot test installation will be pursued. A Wisconsin DOT engineer and member of the advisory panel for this project has already indicated interest in installing this system in his state. A collaborative effort would take place between the research team, Wisconsin DOT personnel, and installers within the state to ensure proper construction and monitoring of the test installations. This will help the research team more fully vet the terminal and adhere to the recommendations in MASH to study field performance. Findings from this pilot study will be published and made available upon request.

In addition, a journal paper will be submitted and, if possible, presented at a TRB annual or summer meeting. Such a presentation would provide the rest of the highway safety industry with the opportunity to interact with the research team and understand what steps were taken to develop a prototype based on the presented findings. As a journal paper, this will have a far reaching effect and may bring about a more rapid evolution in the energy absorbing guardrail terminal market.

7. QUESTIONS FROM REVIEWERS

The research team received comments and questions from reviewers provided by TRB IDEA. The comments were addressed with clarifications made to the body of the text. Questions that were not addressed in the original draft report are paraphrased in this section with the research team's response.

- Is the purpose of this project to develop a commercial product, and if so, can this be provided as standard drawings?
 - The main purpose of this TRB IDEA project was to prove the concept of a non-gating terminal and provide other engineers with the tools and knowledge that will guide them in creating the next wave of advanced terminal technology. Part of the project included a demonstration that the tools and knowledge work. To that end, a prototype was developed and tested. That development has continued outside of the scope of this project. When it is finished, it will be presented to the industry, complete with standard drawings. In the interim, a paper was submitted to TRB before the August 1, 2020 deadline for the 100th Annual TRB Conference.
- Does the added cable increase cost and does the shortened length of the terminal offset this increase?
 - At this stage, it is too early to answer this question completely, but the research team can offer some insight. First, most terminals use a cable, so the cable itself will not increase cost. Its attachment to the rail is different and may change costs. It is welded in place, using swaged buttons as the base material for the weld. There are reinforcement plates on the guardrail as well to distribute the large anchor force over a wider area. However, the overall construction of the first panel of guardrail and the terminal head itself is straight forward and should not increase costs to the point where the reduced length and increased performance cannot offset any possible increases.
- Why was the angle set at 15 degrees?
 - This angle is recommended in MASH for non-gating devices. For the test vehicles, speed, and this angle, the impact condition is generally more severe than 95% of real-world crashes. It is also greater than most impact angles into the end of a terminal in the real world, with larger angles providing much greater overall loading of the terminal. Lower angles, while more common, are also much less of a load and are easier to accommodate. Therefore, 15 degrees was chosen because it is steep enough to significantly load the terminal but shallow enough as to be a reasonable real-world impact condition.

8. REFERENCES

- 1) *Roadside Design Guide*, 4th ed., American Association of State Highway and Transportation Officials, Washington, D.C., 2011.
- 2) *Recommended Procedures for the Safety Performance Evaluation of Highway Features*, NCHRP Report Number 350, Transportation Research Board, National Research Council, Washington, D.C., 1993.
- 3) *Manual for Assessing Safety Hardware*, 2nd ed., American Association of State Highway and Transportation Officials, Washington, D.C., 2016.
- 4) D.L. Sicking, J.R. Rohde, R.K. Faller, and J.C. Holloway, *Crash Testing of Michigan's Type B (W-Beam) Guardrail System – Phase II*, Report TRP-03-104-00, Midwest Roadside Safety Facility, Michigan Department of Transportation, December 13, 2000.
- 5) K.A. Polivka, R.K. Faller, D.L. Sicking, J.R. Rohde, J.D. Reid, and J.C. Holloway, *Guardrail and Guardrail Terminals Installed Over Curbs – Phase II*, Report TRP-03-105-00, Midwest Roadside Safety Facility, Midwest States' Regional Pooled Fund Program, November 5, 2001.
- 6) K.A. Polivka, R.K. Faller, D.L. Sicking, J.R. Rohde, J.D. Reid, and J.C. Holloway, *NCHRP 350 Development and Testing of a Guardrail Connection to Low-Fill Culverts*, Report TRP-03-114-02, Midwest Roadside Safety Facility, Midwest States' Regional Pooled Fund Program, November 1, 2002.
- 7) J.E. Herr, J.R. Rohde, D.L. Sicking, J.D. Reid, R.K. Faller, J.C. Holloway, B.A. Coon, and K.A. Polivka, *Development of Standards for Placement of Steel Guardrail Posts in Rock*, Report TRP-03-119-03, Midwest Roadside Safety Facility, Midwest States' Regional Pooled Fund Program, May 30, 2003.
- 8) B.W. Bielenberg, R.K. Faller, J.R. Rohde, J.D. Reid, D.L. Sicking, and J.C. Holloway, *Development of Tie-Down and Transition Systems for Temporary Concrete Barrier on Asphalt Road Surfaces*, Report TRP-03-180-06, Midwest Roadside Safety Facility, Midwest States' Regional Pooled Fund Program, February 23, 2007.
- 9) K.A. Polivka, R.K. Faller, D.L. Sicking, J.R. Rohde, B.W. Bielenberg, J.D. Reid, and B.A. Coon, *Performance Evaluation of the SKT-MGS Tangent End Terminal – Update to NCHRP 350 Test No. 3-34 (2214TT-1)*, Report TRP-03-176-06, Midwest Roadside Safety Facility, National Cooperative Highway Research Program, October 12, 2006.
- 10) K.A. Polivka, R.K. Faller, D.L. Sicking, J.R. Rohde, B.W. Bielenberg, and J.D. Reid, *Performance Evaluation of the Midwest Guardrail System – Update to NCHRP 350 Test No. 3-10 (2214MG-3)*, Report TRP-03-172-06, Midwest Roadside Safety Facility, National Cooperative Highway Research Program, October 11, 2006.
- 11) E.A. Johnson, D.L. Sicking, R.K. Faller, K.A. Lechtenberg, J.R. Rohde, R.W. Bielenberg, J.D. Reid, and S.K. Rosenbaugh, *Phase I Development of a Non-Proprietary, Four-Cable, High Tension Median Barrier*, Report TRP-03-213-11, Midwest Roadside Safety Facility, Midwest States Regional Pooled Fund Program, December 28, 2011.
- 12) K.D. Schrum, K.A. Lechtenberg, R.W. Bielenberg, S.K. Rosenbaugh, R.K. Faller, J.D. Reid, and D.L. Sicking, *Safety Performance Evaluation of the Non-Blocked Midwest Guardrail System (MGS)*, Report TRP-03-262-11, Midwest Roadside Safety Facility, Midwest States Regional Pooled Fund Program, January 24, 2013.
- 13) D.A. Gutierrez, K.A. Lechtenberg, R.W. Bielenberg, R.K. Faller, J.D. Reid, and D.L. Sicking, *Midwest Guardrail System (MGS) with Southern Yellow Pine Posts*, Report TRP-03-272-13, Midwest Roadside Safety Facility, Midwest States Regional Pooled Fund Program, September 4, 2013.
- 14) J.E. Kohtz, R.W. Bielenberg, S.K. Rosenbaugh, R.K. Faller, K.A. Lechtenberg, and J.D. Reid, *MASH Test Nos. 3-11 and 3-10 on a Non-Proprietary Cable Median Barrier*, Report TRP-03-327-16, Midwest Roadside Safety Facility, Midwest States Pooled Fund Program, May 17, 2016.
- 15) D.T. Meyer, K.A. Lechtenberg, R.K. Faller, R.W. Bielenberg, S.K. Rosenbaugh, and J.D. Reid, *MASH Test No. 3-10 of a Non-Proprietary, High-Tension Cable Median Barrier for use in 6H:1V V-Ditch (Test No. MWP-8)*, Report TRP-03-331-17, Midwest Roadside Safety Facility, Midwest States Pooled Fund Program, May 10, 2017.
- 16) M.A. Pajouh, K.A. Lechtenberg, R.K. Faller, J.C. Holloway, R.W. Bielenberg, S.K. Rosenbaugh, and J.D. Reid, *MASH Test No. 3-10 of a Non-Proprietary, High-Tension Cable Median Barrier for use in 6H:1V V-Ditch (Test No. MWP-9)*, Report TRP-03-360-18, Midwest Roadside Safety Facility, Midwest Pooled Fund Program, May 30, 2018.

- 17) K.A. Polivka, R.K. Faller, D.L. Sicking, J.R. Rohde, B.W. Bielenberg, and J.D. Reid, *Performance Evaluation of the Modified G4(1S) Guardrail – Update to NCHRP 350 Test No. 3-11 (2214WB-1)*, Report TRP-03-168-06, Midwest Roadside Safety Facility, National Cooperative Highway Research Program, October 6, 2006.
- 18) K.A. Polivka, R.K. Faller, D.L. Sicking, J.R. Rohde, B.W. Bielenberg, and J.D. Reid, *Performance Evaluation of the Modified G4(1S) Guardrail – Update to NCHRP 350 Test No. 3-11 with 28” C.G. Height (2214WB-2)*, Report TRP-03-169-06, Midwest Roadside Safety Facility, National Cooperative Highway Research Program, October 9, 2006.
- 19) K.A. Polivka, R.K. Faller, D.L. Sicking, J.R. Rohde, B.W. Bielenberg, and J.D. Reid, *Performance Evaluation of the Midwest Guardrail System – Update to NCHRP 350 Test No. 3-11 (2214MG-1)*, Report TRP-03-170-06, Midwest Roadside Safety Facility, National Cooperative Highway Research Program, October 10, 2006.
- 20) K.A. Polivka, R.K. Faller, D.L. Sicking, J.R. Rohde, B.W. Bielenberg, and J.D. Reid, *Performance Evaluation of the Midwest Guardrail System – Update to NCHRP 350 Test No. 3-11 with 28” C.G. Height (2214MG-2)*, Report TRP-03-171-06, Midwest Roadside Safety Facility, National Cooperative Highway Research Program, October 11, 2006.
- 21) K.A. Polivka, R.K. Faller, D.L. Sicking, J.R. Rohde, B.W. Bielenberg, J.D. Reid, and B.A. Coon, *Performance Evaluation of the Free-Standing Temporary Barrier – Update to NCHRP 350 Test No. 3-11 (2214TB-1)*, Report TRP-03-173-06, Midwest Roadside Safety Facility, National Cooperative Highway Research Program, October 11, 2006.
- 22) K.A. Polivka, R.K. Faller, D.L. Sicking, J.R. Rohde, B.W. Bielenberg, J.D. Reid, and B.A. Coon, *Performance Evaluation of the Free-Standing Temporary Barrier – Update to NCHRP 350 Test No. 3-11 with 28” C.G. Height (2214TB-2)*, Report TRP-03-174-06, Midwest Roadside Safety Facility, National Cooperative Highway Research Program, October 12, 2006.
- 23) R.W. Bielenberg, R.K. Faller, J.R. Rohde, J.D. Reid, D.L. Sicking, J.C. Holloway, E.M. Allison, and K.A. Polivka, *Midwest Guardrail System for Long-Span Culvert Applications*, Report TRP-03-187-07, Midwest Roadside Safety Facility, Midwest States’ Regional Pooled Fund Program, November 16, 2007.
- 24) C.J. Stolle, K.A. Polivka, J.D. Reid, R.K. Faller, R.W. Bielenberg, S.K. Rosenbaugh, D.L. Sicking, and E.A. Johnson, *Determination of the Maximum MGS Mounting Height – Phase 1 Crash Testing*, Report TRP-03-255-12 Revision-1, Midwest Roadside Safety Facility, Midwest States Regional Pooled Fund Program, November 30, 2015.
- 25) N.A. Weiland, J.D. Reid, R.K. Faller, D.L. Sicking, R.W. Bielenberg, and K.A. Lechtenberg, *Minimum Effective Guardrail Length for the MGS*, Report TRP-03-276-13, Midwest Roadside Safety Facility, Wisconsin Department of Transportation, August 12, 2013.
- 26) S.K. Rosenbaugh, R.K. Faller, B.M. Humphrey, T.L. Schmidt, K.A. Lechtenberg, and J.D. Reid, *MASH Test Nos. 3-17 and 3-11 on a Non-Proprietary Cable Median Barrier*, Report TRP-03-303-15, Midwest Roadside Safety Facility, Midwest States Regional Pooled Fund Program, November 3, 2015.
- 27) A.J. Haase, J.E. Kohtz, K.A. Lechtenberg, R.W. Bielenberg, J.D. Reid, and R.K. Faller, *Midwest Guardrail System (MGS) with 6-ft Posts Placed Adjacent to a 1V:2H Fill Slope*, Report TRP-03-320-16, Midwest Roadside Safety Facility, Midwest States Regional Pooled Fund Program, August 22, 2016.
- 28) S.K. Rosenbaugh, R.K. Faller, K.A. Lechtenberg, and J.C. Holloway, *Development and Evaluation of Weak-Post W-Beam Guardrail in Mow Strips*, Report TRP-03-322-15, Midwest Roadside Safety Facility, Midwest States Regional Pooled Fund Program and Mid-America Transportation Center, October 1, 2015.
- 29) J.L. Lingenfelter, S.K. Rosenbaugh, R.W. Bielenberg, K.A. Lechtenberg, R.K. Faller, and J.D. Reid, *Midwest Guardrail System (MGS) with an Omitted Post*, Report TRP-03-326-16, Midwest Roadside Safety Facility, Midwest States Pooled Fund Program, February 22, 2016.
- 30) K.A. Lechtenberg, R.K. Faller, S.K. Rosenbaugh, and J.D. Reid, *Phase III Demonstration of Ponderosa Pine Round Posts as Alternative to Rectangular SYP Posts in G4(2W) Guardrail Systems*, Report TRP-03-329-15, Midwest Roadside Safety Facility, Arizona State Forestry Division and Forest Products Laboratory and Arizona Log & Timberworks, May 17, 2016.
- 31) D.T. Meyer, J.D. Reid, K.A. Lechtenberg, R.W. Bielenberg, and R.K. Faller, *Increased Span Length for the MGS Long-Span Guardrail System Part II: Full-Scale Crash Testing*, Report TRP-03-339-17, Midwest Roadside Safety Facility, Midwest States Pooled Fund Program, April 7, 2017.
- 32) C.J. Stolle, L. Zhu, K.A. Lechtenberg, R.W. Bielenberg, R.K. Faller, D.L. Sicking, J.D. Reid, and J.R. Rohde, *Performance Evaluation of Type II and Type IIA Box Beam End Terminals – Volume 1: Research Results and*

- Discussion*, Report TRP-03-203-10, Midwest Roadside Safety Facility, New York State Department of Transportation, January 20, 2010.
- 33) C.J. Stolle, L. Zhu, K.A. Lechtenberg, R.W. Bielenberg, R.K. Faller, D.L. Sicking, J.D. Reid, and J.R. Rohde, *Performance Evaluation of Type II and Type IIA Box Beam End Terminals – Volume 2: Appendices*, Report TRP-03-203-10, Midwest Roadside Safety Facility, New York State Department of Transportation, January 20, 2010.
- 34) M. Mongiardini, R.K. Faller, J.D. Reid, D.L. Sicking, C.S. Stolle, and K.A. Lechtenberg, *Downstream Anchoring Requirements for the Midwest Guardrail System*, Report TRP-03-279-13, Midwest Roadside Safety Facility, Wisconsin Department of Transportation, October 28, 2013.

9. APPENDIX A – RESULTS OF SINGLE-VARIABLE PARAMETER STUDY

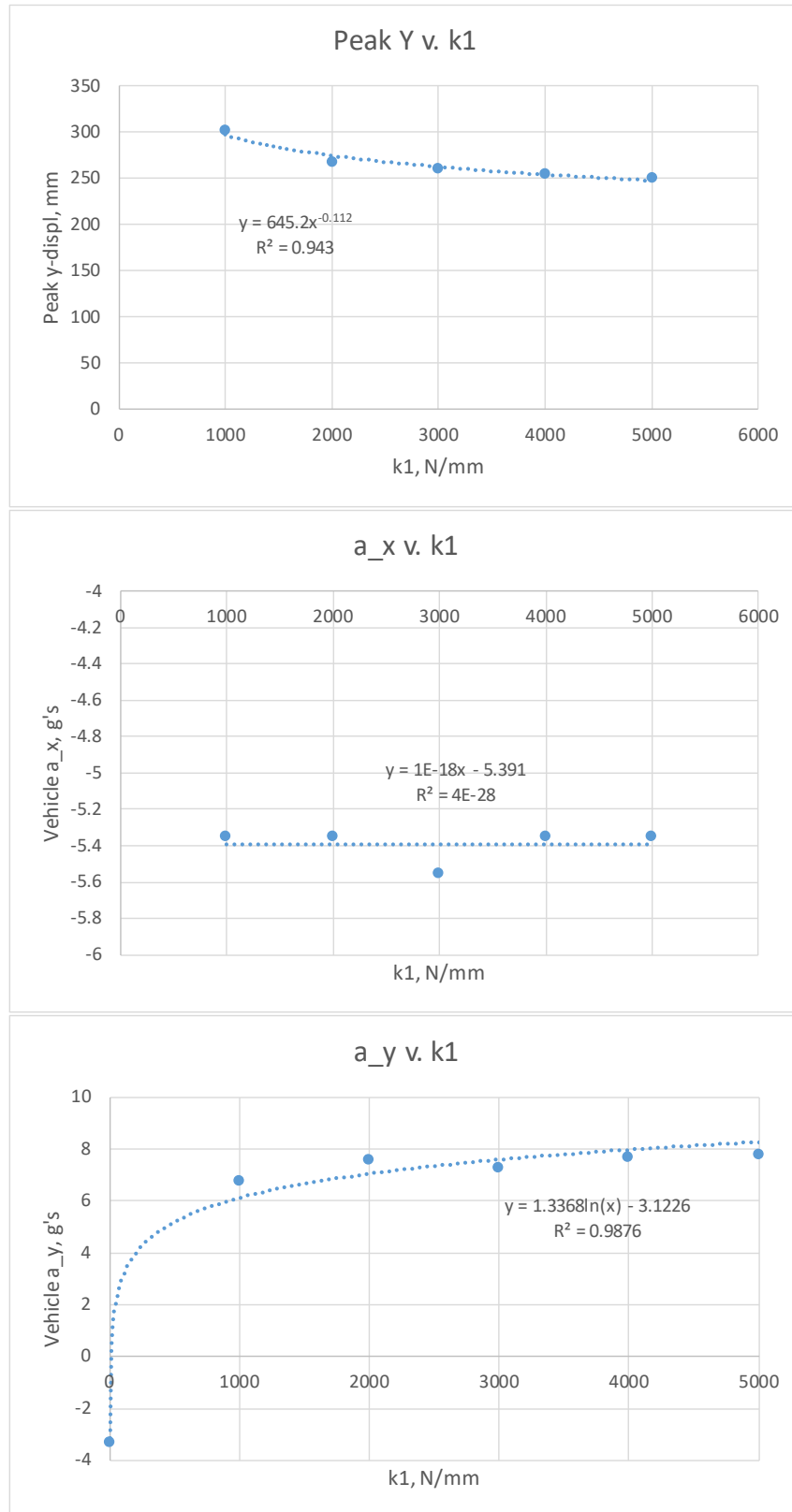


Figure A1. Results of "k1"

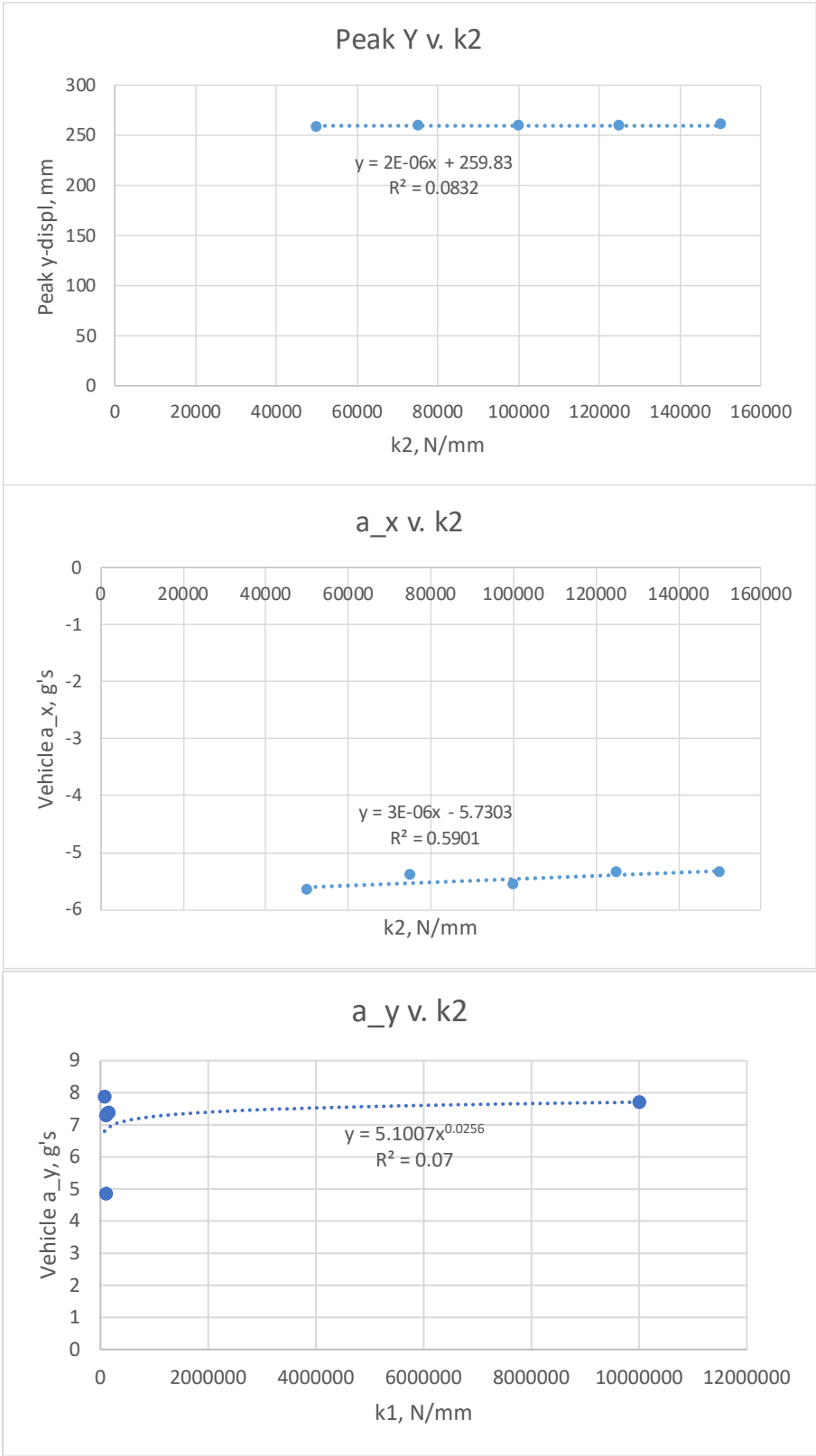


Figure A2. Effect of "k2"

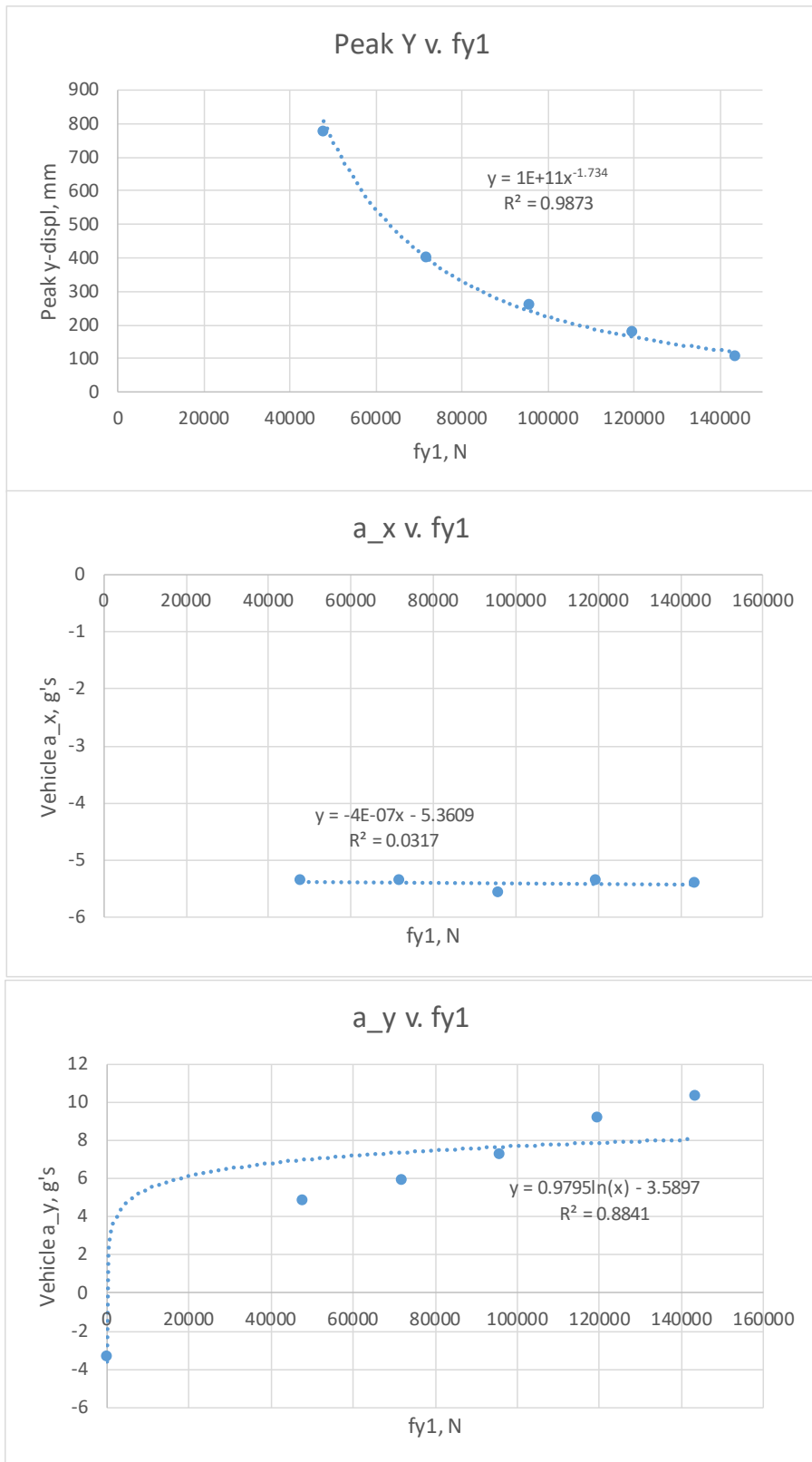


Figure A3.Effect of “fy1”

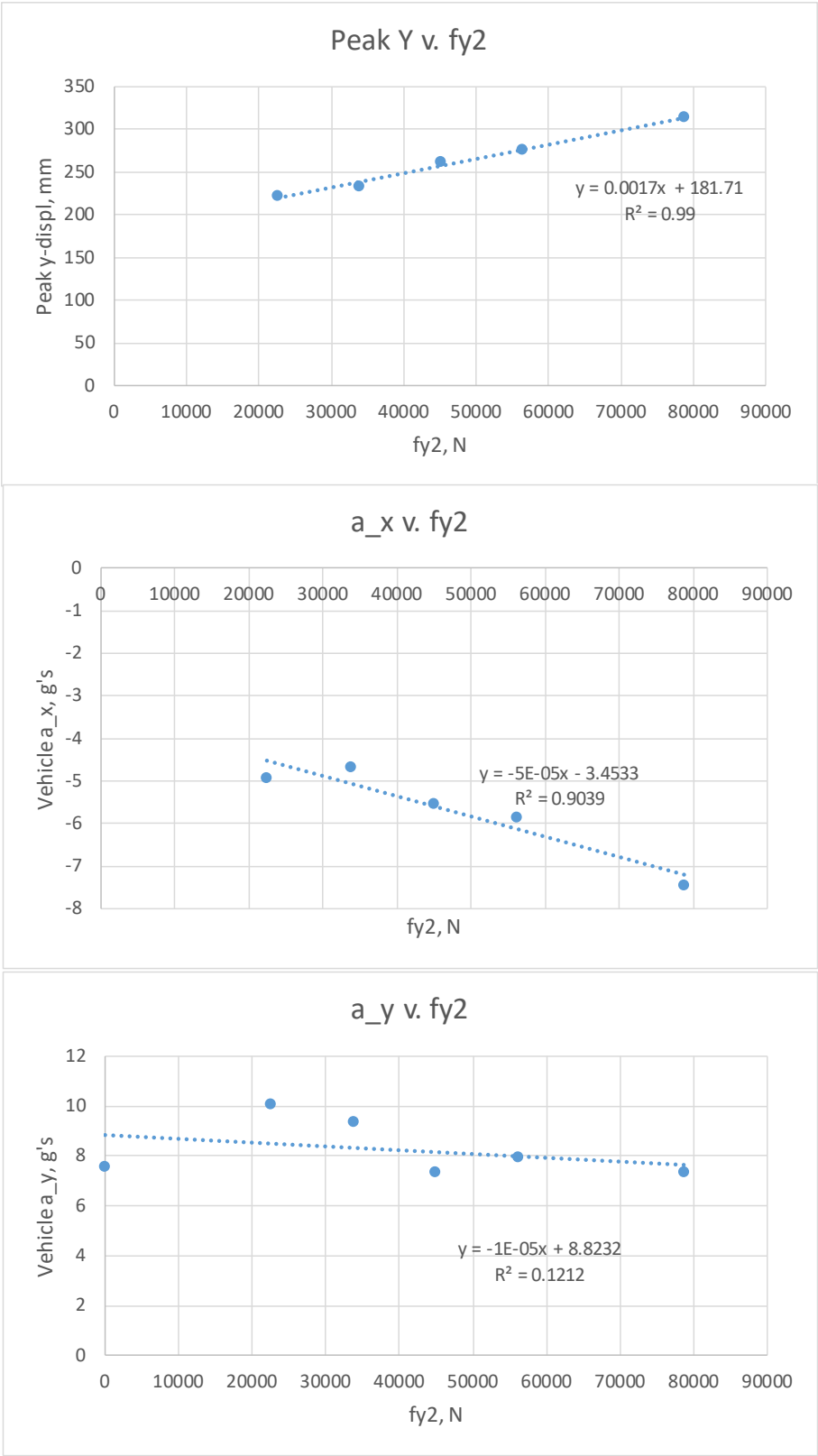


Figure A4. Effect of "fy2"

10. APPENDIX B – RESULTS OF TWO-VARIABLE PARAMETER STUDY

fy1 (kips)	fy2 (kips)	fy2/fy1	V_x	V_y
11	5.058453	0.470514	49.79308	-3.07426
11	7.58768	0.705772	45.28793	-2.81089
11	10.11691	0.941029	41.07194	-2.31815
11	12.64613	1.176286	36.65243	-1.92101
11	17.70459	1.646801	27.798	-1.67718
16	5.058453	0.313676	49.43035	-2.9838
16	7.58768	0.470514	45.04909	-2.46282
16	10.11691	0.627353	40.48646	-1.73722
16	12.64613	0.784191	36.21277	-1.73402
16	17.70459	1.097867	27.4536	-1.07956
22	5.058453	0.235257	49.35878	-3.11729
22	7.58768	0.352886	45.00928	-2.63211
22	10.11691	0.470514	40.66179	-2.57515
22	12.64613	0.588143	35.75409	-1.59558
22	17.70459	0.8234	27.30757	-0.65528
27	5.058453	0.188206	49.29214	-3.17774
27	7.58768	0.282309	44.68501	-2.79559
27	10.11691	0.376412	40.34288	-2.14114
27	12.64613	0.470514	35.85025	-2.15496
27	17.70459	0.65872	27.04681	-1.27122
32	5.058453	0.156838	49.27201	-3.21634
32	7.58768	0.235257	44.54165	-2.80995
32	10.11691	0.313676	40.02867	-2.33022
32	12.64613	0.392095	35.65367	-1.97919
32	17.70459	0.548934	26.63107	-1.50415
32	25.80216	0.8	13.0081	0.622239
32	29.02743	0.9	7.562331	0.694952
32	32.2527	1	1.737151	1.433578
16	24.18952	1.5	16.01677	0.103532

Figure B1. Tabulated Results of the Two-Variable Parameter Study

11. APPENDIX C – RESULTS OF TWO-VARIABLE PARAMETER STUDY

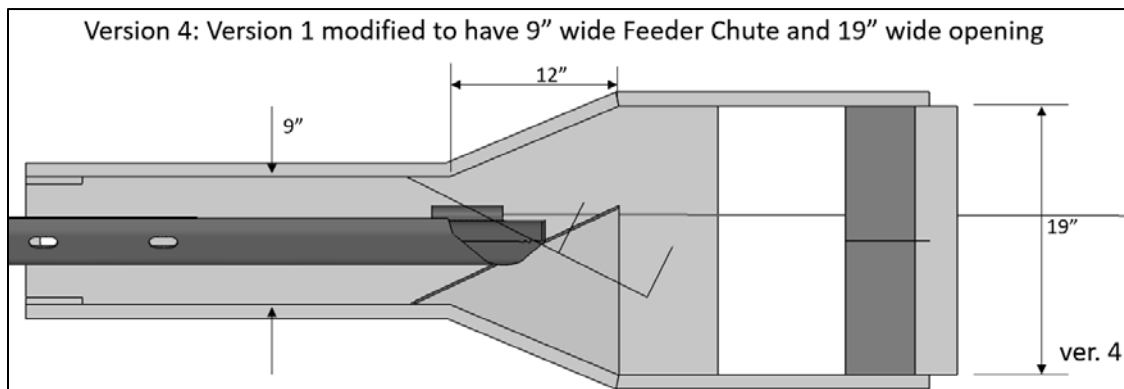
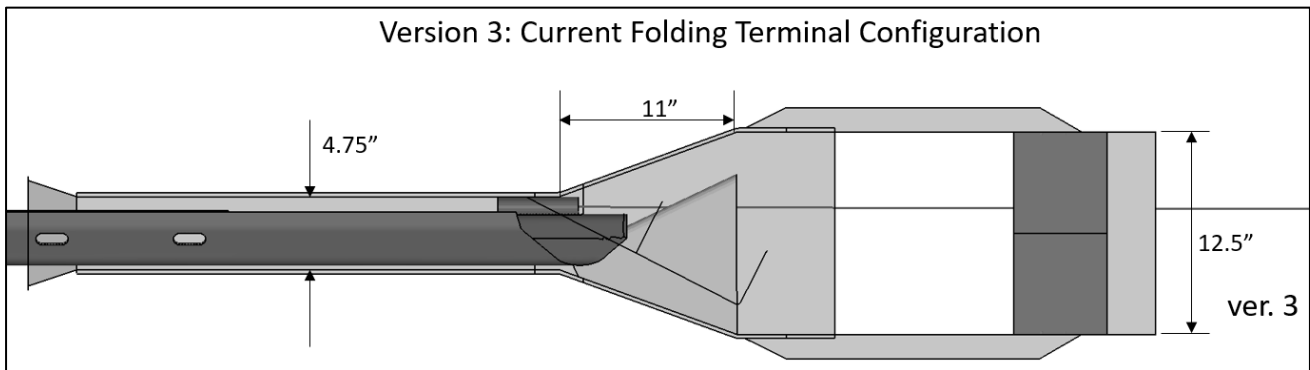
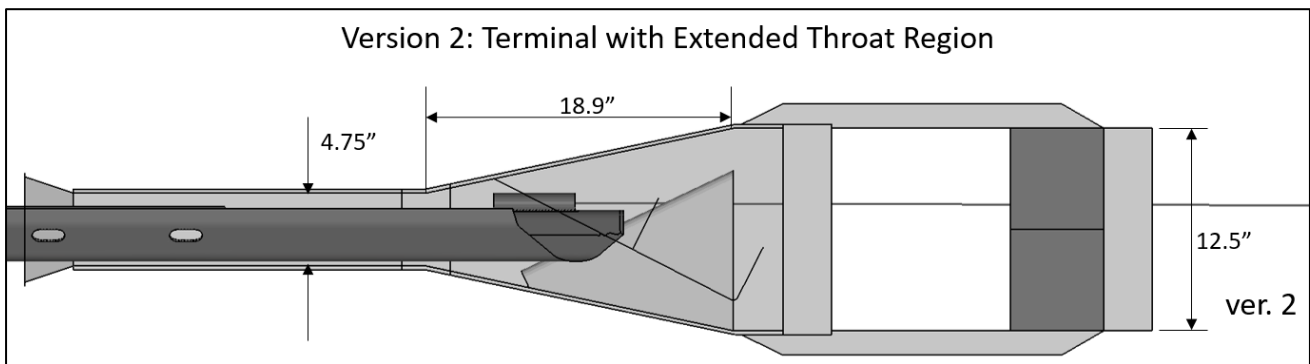
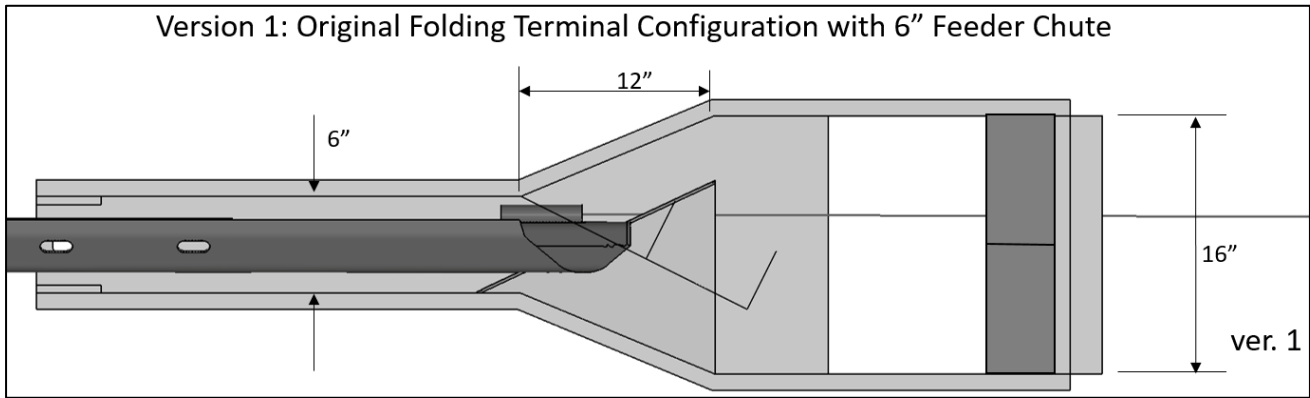


Figure C1. Variations of Terminal Head in Full-Scale Simulations

12. APPENDIX D – RESEARCH RESULTS

Sidebar Info

Program Steering Committee: TRB IDEA Program Committee

Month and Year: April 2020

Title: Non-Gating Guardrail Terminal

Project Number: 212

Start Date: October, 29, 2018

Completion Date: April, 15, 2020

Product Category: Guardrail Terminal

Principal Investigator:

Dean Sicking, Managing Partner, Sicking Safety Solutions, LLC

E-Mail: sickingsafety@gmail.com

Phone: 402-450-6295

TITLE:

Developing Non-Gating Terminals

SUBHEAD:

A guide and example for designing next-generation guardrail terminals

WHAT WAS THE NEED?

Guardrail terminals have evolved over time, with large steps taken when significant shortcomings were addressed. The first was the Turned Down system, which eliminated penetrations but introduced other significant problems. Throughout this long history, every new terminal design concept maintained at least one common feature: they all allowed the errant vehicle to gate through the barrier, unimpeded, for end-on, angled hits. To accommodate this seemingly inherent feature, guardrail installations extend well past the hazard that is being shielded. This places a strain on State budgets. It also requires more labor, which exposes construction crews to dangerous traffic conditions. Finally, with additional length of guardrail, itself being a fixed object and a hazard, the number of crashes increases relative to a shorter length of barrier. One way to address many of these issues is to use flared terminals. However, very few flared terminals are available on the market that absorb energy. Also, they require much more work to grade a larger portion of the roadside in accordance with the installation manuals. This increases cost, thus negating the benefit of a shorter installation in terms of funding. Therefore, a new concept of guardrail terminal is needed. One that can maintain tension throughout an impact while preventing angled impacts from gating through.

WHAT WAS OUR GOAL?

The objective of this research was to identify the critical design elements, such as lateral and longitudinal forces imparted on the vehicle by the terminal that results in a non-gating performance. An additional objective was to design, build, and test a prototype to prove the concept of a non-gating guardrail terminal.

WHAT DID WE DO?

This research was conducted in three phases. In the first phase, existing research was identified that included guardrail redirection tests, such as Test No. 3-11 in either NCHRP 350 or MASH. The peak forces and lateral displacements were

recorded and compared. Using this comparison, a baseline was observed for a successful redirection test when the face of the guardrail is struck. This finding was a starting point for the second phase.

In the second phase, a simple and a complex computer model were created. The simple model involved springs that were adjustable. One spring applied a force along the length of the terminal (a longitudinal force), and another spring applied a force perpendicular to the barrier (a lateral force). Using this simple model, the combinations of longitudinal forces and lateral forces were studied, and it was observed that for one given force, the other must fall within a range. If it is outside this range, either below or above, it will allow the vehicle to gate. The complex model was built on the same principle but used the geometry of an energy absorbing terminal head, currently under development by the research team. This step showed that the abstract forces from the simple model can translate to existential forces in the form of post cross-section and terminal head geometry.

In the final stage, a prototype was designed, built, and tested at the research team's test facility. The design was largely based on the simulation results of the complex model. In this effort, two full-scale crash tests were conducted, each at 15 degrees with the terminal head striking the center of each vehicle. The first test was a Ford Explorer at 50 mph, and the second test was a Mazda Protégé at 64 mph. The forward velocity of both vehicles was completely stopped, and the terminal head remained engaged with both vehicles up until the forward velocity was stopped. Both tests would have passed the MASH criteria.

Engineers from the Alabama, Wisconsin, and Wyoming Departments of Transportation served as advisory panel members. They provided their own insights at the beginning of the project, as well as at the end. Collaborative efforts to study the field performance of this device are under discussion with the Wisconsin DOT.

WHAT WAS THE OUTCOME?

A literature review of crash tests involving a full length of guardrail found that the minimum redirecting force was 21.5 kips with a maximum deflection of 5 feet. This was a good starting point to help build a simple spring model, but it was soon apparent that the W-beam barrier in length-of-need tests greatly benefitted from having an upstream and a downstream portion of guardrail. This is not possible for a terminal. The model was tuned to account for a lack of guardrail, with the expectation that the guardrail would have to be continually anchored (i.e., a tension-based design). Models indicated that for a given longitudinal force, there was a range of lateral forces that would permit non-gating, and this lateral force could take the form of a plastic section modulus of the posts. Finally, with this knowledge, a prototype was built that successfully arrested the forward velocity of two different vehicles while maintaining connection and not allowing the vehicles to pass beyond the terminal head.







WHAT IS THE BENEFIT?






This proof-of-concept should provide manufacturers with confidence that a non-gating system can be developed, and it should provide increased budgetary freedom and overall public safety for State DOTs. Shorter lengths of guardrail are less expensive to install and take less time. This creates less exposure of construction crews to dangerous traffic conditions and minimizes the length of a hazard (the guardrail itself) to the motoring public, all while requiring no more grading than a typical tangent terminal.

LEARN MORE

<Provide link to final report or other pertinent info, such as how to access an online tool.>

IMAGES

Time (msec)	Ford Explorer
0	 A dark blue Ford Explorer is shown from a high-angle perspective, positioned on a concrete test track. The vehicle is facing right, and its shadow is cast to the left. A green obstacle is visible on the left side of the track.
120	 The Ford Explorer is shown at 120 msec, beginning to rotate clockwise. The front end is slightly turned towards the right.
240	 At 240 msec, the Ford Explorer is more rotated. The front end is significantly turned towards the right, and some debris is visible on the ground.
360	 At 360 msec, the Ford Explorer is further rotated. The front end is almost perpendicular to the track's direction.
480	 At 480 msec, the Ford Explorer is nearly fully rotated. The front end is almost directly facing the camera.
600	 At 600 msec, the Ford Explorer is fully rotated and is now facing the camera directly.

Time (msec)	Mazda Protégé
0	 A silver Mazda Protégé is shown from a high-angle perspective, positioned on a concrete test track. The vehicle is facing right, and its shadow is cast to the left. A green obstacle is visible on the left side of the track.
120	 At 120 msec, the Mazda Protégé is shown beginning to rotate clockwise. The front end is slightly turned towards the right.
240	 At 240 msec, the Mazda Protégé is more rotated. The front end is significantly turned towards the right, and some debris is visible on the ground.
360	 At 360 msec, the Mazda Protégé is further rotated. The front end is almost perpendicular to the track's direction.
480	 At 480 msec, the Mazda Protégé is nearly fully rotated. The front end is almost directly facing the camera.